



TECHNICAL UNIVERSITY OF CRETE
SCHOOL OF PRODUCTION
ENGINEERING AND MANAGEMENT

**Evaluation of a model predictive control strategy on a
calibrated multilane microscopic model**

Georgia Perraki

Supervisor: Prof. Ioannis Papamichail

Thesis submitted in partial fulfillment of the requirements for the degree of
Master of Science

Chania, Greece, 2016

Acknowledgments

This thesis would not have been possible without the valuable contribution and guidance of certain people. Firstly, I would like to thank Dr. Claudio Roncoli who has supported me throughout my thesis with his patience and knowledge. I am also thankful to Associate Professor Ioannis Papamichail for his supervision, trust and valuable advices. Moreover, I would like to express my gratitude to Professor Markos Papageorgiou whose guidance inspired me to develop an understanding and interest on the field of transportation.

Last, but not least i would like to thank my parents, my sisters and my boyfriend for their love, support and encouragement all these years.

This master thesis has been conducted in the frame of the project TRAMAN21, which has received funding from the European Research Council under the European Union's Seventh Framework Programme (FP/2007-2013)/ERC Advanced Grant Agreement n. 321132.



Abstract

This master thesis investigates the effectiveness of a Model Predictive Control (MPC) scheme applied on a calibrated and validated microscopic multilane model. Microscopic traffic models have become increasingly popular in order to solve design and analysis problems difficult to be studied by other means. Although the simulation models can be useful for engineers, they have to be firstly calibrated and validated in order to ensure that they can lead to meaningful results. A stretch of the freeway A20 which connects Rotterdam to Gouda in the Netherlands is modeled in a microscopic simulator. Speed and flow measurements, collected from the field, are used in order to tune the simulation parameters with the purpose of replicating realistic traffic conditions. Different datasets are used in order to verify that the model reproduces reality under different conditions. An MPC scheme is then applied in the calibrated model aiming at the mitigation of traffic congestion in the case study network. The control strategy is based on the assumption that the vehicles are equipped with Vehicle Automation and Communication Systems (VACS), which offer numerous advantages concerning the actuation possibilities and availability of information.

Keywords: Microscopic simulation, AIMSUN, Calibration, Validation, MPC, VACS

Contents

1	Introduction	1
1.1	Motivation	1
1.2	Thesis objectives	2
1.3	Thesis outline	3
2	Calibration of microscopic simulation models	4
2.1	Literature review	4
2.2	The AIMSUN microscopic simulator	6
2.2.1	Introduction	6
2.2.2	Behavioral models	7
2.2.3	Car-following model	7
2.2.4	Lane-changing model	9
2.2.4.1	Gipps lane-changing model	10
2.2.4.2	Heuristic rules on lane-changing model	11
2.3	Calibration and validation processes	12
2.3.1	Calibration process	13
2.3.1.1	Calibration parameter selection	14
2.3.1.2	Optimal parameter setting	17
2.3.2	Validation process	20
3	Model predictive control for multilane motorway traffic	21
3.1	Literature review	21

3.2	Methodology	23
3.2.1	Multi-lane macroscopic traffic flow model	24
3.2.2	Optimization problem	26
3.2.3	Control structure	32
4	Results	36
4.1	Experimental setup	36
4.1.1	Test site and data	36
4.1.2	Real traffic conditions	39
4.1.3	Dynamic scenario	44
4.2	Calibration and validation	45
4.2.1	Parameter setup	45
4.2.2	Calibration results	48
4.2.3	Validation results	53
4.3	Application of model predictive control	57
4.3.1	Optimization problem setup	57
4.3.2	Calibrated scenario results	60
4.3.3	Validated scenario results	69
5	Conclusions and future work	71
5.1	Conclusions	71
5.2	Future work	72

List of Figures

2.1	Heuristic rules replacing the lane-changing model based on current speed (red line), distance (blue line) and speed difference (green line).	11
2.2	Methodology for optimization based model calibration	19
3.1	The segment-lane variables used in the model formulation	25
3.2	The proposed FD including both the demand and the supply piecewise-linear functions.	26
3.3	Proposed control framework	32
4.1	Test site network	37
4.2	Locations of spot detectors placed at each lane of the network	39
4.3	Real data speed, Monday 26-01-2009	40
4.4	Real data speed, Thursday 02-04-2009	40
4.5	Real data speed, Tuesday 12-05-2009	40
4.6	Real data speed, Monday 08-06-2009	41
4.7	Real data speed, Thursday 25-06-2009	41
4.8	Real data speed, Wednesday 26-05-2010	41
4.9	Real data speed, Monday 21-06-2010	42
4.10	Heuristic lane-changing rules applied in the acceleration lane	47
4.11	Heuristic lane-changing rules applied in the lane drop	48
4.12	Real data speed, Wednesday 26-05-2010	49
4.13	Simulated speed, Wednesday 26-05-2010	49

4.14 Comparison between measured (blue line) and simulated (red line) aggregate flow at detector locations 1-4	50
4.15 Comparison between measured (blue line) and simulated (red line) aggregate flow at detector locations 5-8	50
4.16 Comparison between measured (blue line) and simulated (red line) aggregate flow at detector locations 9-12	51
4.17 Comparison between measured (blue line) and simulated (red line) aggregate flow at detector locations 13-16	51
4.18 Comparison between measured (blue line) and simulated (red line) aggregate flow at detector locations 17-20	52
4.19 Comparison between measured (blue line) and simulated (red line) aggregate flow at detector locations 21-24	52
4.20 Real data speed, Monday 08-06-2009	54
4.21 Simulation speed, Monday 08-06-2009	54
4.22 Real data speed, Thursday 25-06-2009	55
4.23 Simulated speed, Thursday 25-06-2009	55
4.24 Real data speed, Monday 21-06-2010	56
4.25 Simulation speed, Monday 21-06-2010	56
4.26 Schematic representation of the case study network discretized in 21 segments	57
4.27 Piecewise linear FDs for segment 8 - lane 2 (right) and for the rest of the network (left)	60
4.28 Time-accumulated time spent in the control case (blue line) and the no-control case (red line).	61
4.29 No-control case speed, Wednesday 26-05-2010	62
4.30 Control case speed, Wednesday 26-05-2010	62
4.31 Comparison between the aggregate flow in the control (red line) and no-control cases (blue line) at segments 10-13	63

4.32 Comparison between the requested (red line) and the accomplished (blue line) right lateral movement segment 6 65

4.33 Comparison between the requested (red line) and the accomplished (blue line) right lateral movement segment 7 65

4.34 Comparison between the requested (red line) and the accomplished (blue line) left lateral movement segments 9 & 15 65

4.35 Comparison between the requested (red line) and the accomplished (blue line) speed limits in segment 6 66

4.36 Comparison between the requested (red line) and the accomplished (blue line) speed limits in segment 7 66

4.37 Comparison between the requested (red line) and the accomplished (blue line) speed limits in segment 8 67

4.38 Comparison between the expected (red line) and the measured (blue line) longitudinal flow in segment 6 67

4.39 Comparison between the expected (red line) and the measured (blue line) longitudinal flow in segment 7 67

4.40 Comparison between the expected (red line) and the measured (blue line) longitudinal flow in segment 8 68

4.41 Comparison between the requested (red line) and the accomplished (blue line) inflow from on-ramps 1 & 2 68

4.42 Time-accumulated time spent in the control case (blue line) and the no-control case (red line) on Monday 08-06-2009 69

4.43 No-control case speed, Monday 08-06-2009 70

4.44 Control case speed, Monday 08-06-2009 70

List of Tables

4.1	Available real data for the test site network	38
4.2	Mean, deviation, minimum and maximum values of calibrated key parameters	45
4.3	Values of manually calibrated parameters	46
4.4	Weight parameters of the quadratic terms	58
4.5	Coefficient for right and left lateral movement	59
4.6	Values of upper and lower bounds	59

Chapter 1

Introduction

1.1 Motivation

Nowadays traffic congestion in most countries is increasing and the extent of the effects heavy traffic can have must be taken under consideration in order to improve the quality of life in big cities. Some possible ways to reduce the consequences of the traffic jams could be the building of new road infrastructures, the introduction of more strict pricing policies, the promotion of public transportation and so on. On the contrary, the currently existing motorways are actually underutilized, especially in the period of high demand (Papageorgiou et al., 2003). The degradation and underutilization of the freeway networks which accordingly lead to reduced throughput in periods of congestion can be countered via suitable control measures and strategies (Papageorgiou, 2004).

In the last two decades, a significant and increasing interdisciplinary effort by the automotive industry, as well as by numerous research institutions around the world, has been devoted to the planning, developing, testing and deploying a variety of Vehicle Automation and Communication Systems (VACS) that are expected to revolutionize the features and capabilities of individual vehicles within the next decades (Roncoli et al., 2014). Although it is proved that VACS may affect the traffic flow on a motorway system both positively and negatively, their appropriate employment in traffic management techniques may be beneficial since they can offer the possibility of having access to control actions that are

not available with conventionally driven cars (e.g., individual vehicle speed or lane-change advices). The current penetration level of VACS is very limited. Thus, their study is performed either via Field Operational Tests (FOTs), which mainly concern technological aspects, safety effects, changes in driving behavior, user acceptance, and environmental impacts or via simulation investigations which are used to reveal their traffic flow implications (Diakaki et al., 2015).

Microscopic simulation models have been widely used in both transportation operations and management analyses because simulation is safer, less expensive, and faster than field implementation and testing (Park, 2006). Some of the most commonly used commercial vehicular microscopic simulation models are AIMSUN (Transport Simulation Systems, 2014), VISSIM (PTV Planug Transport Verkehr AG. Innovative Transportation Concepts LLC, 2001), CORSIM (FHWA, U.S. Department of Transportation, 1997), etc. In order to provide reliable results the simulation models must be initially calibrated and validated for the specific study network and the future traffic management actions. In the traditional process of model calibration, model parameters are adjusted until reasonable (qualitative and quantitative) correspondence between the model and field observed data is achieved. Such adjustments with multiple parameters are a time consuming and tedious process. The trial-and-error method based on engineering judgment or experience is usually employed for model calibration while more systematic approaches include optimization-based techniques like Genetic Algorithms (GA) (Goldberg, 1989) or the Nelder-Mead algorithm (Lagarias et al., 1998) as in the works of (Chu et al., 2004) and (Spiliopoulou et al., 2014) respectively. Because the calibration of microscopic simulation models is considered as time consuming and computation intensive process one might resort to using the model without calibrating it first which rarely leads to reliable results.

1.2 Thesis objectives

The objective of this work is to represent the application of microsimulation in a part of the freeway A20 in the Netherlands. The microscopic model is calibrated and validated

based on a process that involves manual tuning and optimization based techniques. Real traffic data is used in order to build the simulation scenario and to evaluate the simulation output. Once a reliable model is developed a Model Predictive Control (MPC) strategy is applied in order to mitigate the traffic congestion of the motorway. The control scheme, proposed and tested in (Roncoli et al., 2014) using a microscopic model of a small freeway stretch, takes into account the use of VACS which offers increased degrees of freedom concerning not only the control possibilities but also the information needed to determine the motorway state. The core of the methodology is the convex optimization problem proposed in (Roncoli et al., 2015b), that is based on the piecewise linear macroscopic traffic flow model (Roncoli et al., 2015a), which already considers, as decision variables, actions that are enabled with the aid of VACS.

1.3 Thesis outline

This master thesis is composed of five chapters. Chapter 2 starts with a literature review on previous studies in calibration of microscopic models while subsequently a brief description of the AIMSUN microscopic simulator and the employed behavioral models follows. Afterwards the calibration and validation processes are presented. In Chapter 3, a number of reviewed studies in traffic control strategies are briefly described and then the proposed MPC strategy is expounded. Chapter 4 consists of a detailed representation of the test site network, the available observed data from the field and the real traffic conditions appearing at certain days. Subsequently, the calibration and validation results are presented based on a comparison of the simulation output and the real data observations. The setup of the MPC strategy is specified and the results of the employed control actions on the calibrated and one of the validated simulation scenarios are shown. Finally, Chapter 5 summarizes the conclusions and also suggests recommendations and potential improvements for future research.

Chapter 2

Calibration of microscopic simulation models

2.1 Literature review

Due to the great importance of the calibration and validation of microscopic models, there have been several studies in the literature related to this subject. This section summarizes a number of the reviewed relevant studies in this field.

Park and Qi (2005) proposed a calibration procedure which aimed to find the best suited values with the application of a genetic algorithm (GA). The validity of the proposed scheme was examined in an actuated signalized intersection by using the VISSIM microscopic model. This calibration and validation process was also evaluated by Park (2006) where the case study network was a work zone and the performance index was the simulation outputs and field travel time data. In both cases, it was concluded that the proposed strategy could lead to model parameters that can efficiently replicate reality.

Chu et al. (2004) presented a systematic procedure composed of several stages for the calibration and validation of the PARAMICS simulation model. In particular, the calibration of the microscopic model is based on the calibration of driving behavior and route choice models, the Origin Destination (OD) estimation and the model fine-tuning. The proposed method was tested in a corridor network in the southern California and it resulted in reasonable performance in replicating the observed flow condition.

Liu et al. (2006) introduced a hybrid heuristic algorithm as an optimization method for microscopic model calibration. The hybrid method combines the Genetic Algorithm (GA) and Simulated Annealing (SA) in order to incorporate the local stochastic hill climbing SA and the global crossover and mutation operating GA. This approach was tested in an urban downtown road network modeled in VISSIM and it was proved that the resulted calibrated parameters could reasonably reproduce the real traffic flow.

In Hourdakis et al. (2003) the authors proposed the calibration of microscopic simulation models with a process based on two trial and error stages. The first stage concerns the volume-based calibration which targets to obtain simulated mainline station volumes as close as possible to the actual mainline station volumes. Subsequently, speed-based calibration follows with the objective of minimizing the discrepancies between the simulated and the actual mainline speeds. The goodness-of-fit statistical measures that were used in the aforementioned approach include RMSEP (Root Mean Squared Error Percent) and the correlation coefficient. The calibration methodology was used in a real life project for a number of freeway sections in Minneapolis, Minnesota and the used simulator was AIMSUN.

Zhizhou et al. (2005) also used a Genetic Algorithm (GA) based optimization approach to find an optimal combination of VISSIM parameters for an expressway model in Shanghai. The authors conducted a sensitivity analysis in order to determine which model parameters have the greatest impact in the speed and volume of the network. Desired speed in reduced speed area, desired lane-change distance, average desired distance between stopped cars and the safety distance are some of the most influential model parameters. GA optimization is implemented and aim to minimize the root mean square error (RMSE) between the simulated and real values of speed and volume. Authors indicated that this method could lead to more accurate results compared to the default set of parameters.

In (Toledo et al., 2003) the calibration and validation of MITSIMLab tool consists of the calibration of driving behavior models and the calibration of origin-destination flows

and route choice models. The test site network was a mixed urban-freeway network while aggregate flow and speed measurements from the field were used for the calibration of the different components of the microscopic model. Different real data measurements retrieved one year later were used in order to test the validity of the calibrated model.

2.2 The AIMSUN microscopic simulator

2.2.1 Introduction

AIMSUN (Advanced Interactive Microscopic Simulator for Urban and Non-urban Networks) (Transport Simulation Systems, 2014) is a commercial microscopic traffic simulation software widely used nowadays by transport professionals and researchers. The system provides highly detailed modeling of the traffic network, it distinguishes between different types of vehicles and drivers, it enables a wide range of network geometries to be dealt with, and it can also model incidents, conflicting manoeuvres, etc. Most traffic equipment present in a real traffic network is also modeled in the microsimulator, e.g. traffic lights, traffic detectors, Variable Message Signs, ramp metering devices.

The input data required by AIMSUN dynamic simulator is a simulation scenario, and a set of simulation parameters that define the experiment. The scenario is composed of four types of data: network description, traffic control plans, traffic demand data and public transport plans. The simulation parameters are fixed values that describe the experiment (such as simulation time, warm-up period, statistics intervals) and some variable parameters used to calibrate the models that include reaction times, lane-changing zones and so forth (Transport Simulation Systems, 2014). Other input data may include, for example, control plans for signalized intersections or information about stop or yield signs at uncontrolled intersections. Common output is macroscopic measures such as average traveling time and speed.

For the users of AIMSUN there is also available the tool of AIMSUN Application Programming Interface (API) that gives them the opportunity to increase the understanding

of the use of probe vehicle data, available applications, visualizations, performance measures and management techniques. Apart from the API tool, the advanced AIMSUN edition includes the AIMSUN microSDK component which has the aim of enabling the integration of new behavioral models and overwriting the models offered by default in the microsimulator. The user has the chance to choose the behavioral models that will be implemented which can be either applied globally to the whole network or locally to a subset of specific sections, and for the remaining to use the default models implemented in AIMSUN.

2.2.2 Behavioral models

Traffic microsimulation models consists of a number of sub-models that aim to approach different aspects of human driver behavior while the accuracy of these models depends highly on the quality of the traffic-flow models (Panwai and Dia, 2005). Some of the most important individual vehicle behavioral models are the car-following model, lane-changing, Gap-Acceptance, on-ramp model and overtaking model. A Gap-Acceptance model is used to approach give way behavior and determines whether a lower priority vehicle approaching an intersection can or cannot cross depending on the circumstances of higher priority vehicles while an on-ramp model defines the lane-changing behavior applied inside on-ramps. Nevertheless, the two main critical components of a traffic simulation system are the car-following and lane-changing models.

2.2.3 Car-following model

Microscopic traffic models describe the motion of each individual vehicle, i.e., they model actions such as accelerations and decelerations of each driver as a response to the surrounding traffic by means of an acceleration strategy towards a desired velocity in the free-flow regime, a braking strategy for approaching other vehicles or obstacles, and a car-driving strategy for maintaining a safe distance when driving behind another vehicle. Microscopic

traffic models typically assume that human drivers react to the stimulus from neighboring vehicles with the dominant influence originating from the directly leading vehicle known as “follow-the-leader” or “car-following” approximation (Kesting and Treiber, 2008).

The AIMSUN microscopic simulator uses a car-following model that is based on the Gipps model (Gipps, 1981). It has been observed, though, that this model does not reproduce capacity drop phenomena realistically (Wang et al., 2005). Due to that, the Intelligent Driver Model (IDM) (Treiber et al., 2000) is implemented and replaces the aforementioned default car-following model, since capacity drop will be a key issue of this work.

The IDM car-following model, is formulated as an ordinary differential equation and, consequently, space and time are treated as continuous variables. This model class is characterized by an acceleration function that depends on the actual velocity $v(t)$, the (net distance) gap $s(t)$ and the velocity difference $\Delta v(t)$ to the leading vehicle:

$$\dot{v}(s, v, \Delta v) = f(s, v, \Delta v) \quad (2.1)$$

The acceleration equation that describes the IDM car-following model is the following:

$$\dot{v}(s, v, \Delta v) = a[1 - (\frac{v}{v_o})^4 - (\frac{s^*(v, \Delta v)}{s})^2], \quad (2.2)$$

This equation consists of two parts. The $\dot{v}_{free}(v) = a[1 - (\frac{v}{v_o})^4]$ which defines the speed based on the maximum desired speed v_o on a free road with the parameter a being the maximum acceleration and the $\dot{v}_{brake}(s, v, \Delta v) = -a(s^*(v, \Delta v)/s)^2$ which dominates if the current gap $s(t)$ to the preceding vehicle becomes smaller than the desired minimum gap defined by the Equation:

$$s^*(v, \Delta v) = s_o + vT + \frac{v\Delta v}{2\sqrt{ab}}, \quad (2.3)$$

where b is the comfortable deceleration, s_o is the minimum bumper-to-bumper distance to the front vehicle and T is the desired safety time headway when following other vehicles.

The minimum distance s_o in congested traffic is significant for low velocities only. The dominating term of Equation (2.2) in stationary traffic is vT which corresponds to following the leading vehicle with a constant desired (safety) time gap T . The last term is only active in non-stationary traffic and implements an “intelligent” driving behavior including a braking strategy that, in nearly all situations, limits braking decelerations to the comfortable deceleration b . Note, however, that IDM brakes stronger than b if the gap becomes too small. This braking strategy makes IDM collision-free. All IDM parameters v_o , T , s_o , a and b are defined by positive values (Kesting and Treiber, 2008).

2.2.4 Lane-changing model

The transfer of a vehicle from one lane to the adjacent has a significant impact on traffic flow. Lane-changing models are therefore an important component in microscopic traffic simulators, which are as mentioned above, the tool of choice for a wide range of traffic-related applications at the operational level. Modeling the behavior of a vehicle within its present lane is relatively straightforward, as the only variables that matter are the speed and location of the preceding vehicle. Lane-changing behavior is something extremely difficult to be modeled mostly due to the numerous factors that influence the decision of the driver to change lane (*Mathew, Tom V. "Lane Changing Models." Lecture, February 19, 2014*).

The default lane-changing model utilized in the AIMSUN microscopic simulator is a development of the Gipps lane-changing model (Gipps, 1986). However, the fact that this model cannot capture the merging behavior in a critical flow regime (Chevallier and Leclercq, 2009) has led us to replace it with heuristic rules that were introduced in (Roncoli et al., 2014). These rules are applied in the sections where the default model is unable to provide good performance while in the rest part of the network the Gipps lane-changing model is being used instead.

2.2.4.1 Gipps lane-changing model

Lane change is modeled as a decision process, analyzing the necessity of the lane change (such as for turning manoeuvres determined by the route), the desirability of the lane change (e.g. to reach the desired speed when the leading vehicle is slower), and the feasibility conditions for the lane change that are also local and depend on the location of the vehicle in the road network (Transport Simulation Systems, 2014).

Each time a vehicle has to be updated, the necessity of a possible lane-changing is wondered. This depends on several factors like the turning feasibility in the current lane, the distance to the next turn and the traffic conditions in the current lane. The traffic conditions are measured in terms of speed and queue lengths. When a driver is going slower than he wishes, he tries to overtake the preceding vehicle. On the other hand, when he is traveling fast enough, he tends to go back into the slower lane. In case that a lane change action is considered necessary, the desirability of this action is determined by evaluating the possible improvement in the traffic conditions for the driver as a result of it. The feasibility of a lane change is taken into account by testing if there is enough gap to safely move to the neighboring lane.

The lane-changing decisions are made based on the classification of the location of the vehicle into one of three zones, with each zone corresponding to a different rank of lane-changing motivation. The zones are:

- Zone 1: The lane-changing decisions are mainly governed by the traffic conditions of the lanes involved. Desired speed of driver, speed and distance of current preceding vehicle, speed and distance of future preceding vehicle in the destination lane are some of the variables that affect the lane-changing decisions within this zone.
- Zone 2: This is the intermediate zone. Vehicles not driving in valid lanes (i.e. lanes where the desired turning movement can be made) tend to get closer to the correct side of the road from which the turn is allowed. Vehicles looking for a gap try to adapt to gaps located either downstream or adjacent.

- Zone 3: Vehicles are forced to reach their valid lane, looking for gaps upstream and reducing speed if necessary, even coming to a complete stop in order to make the change possible.

2.2.4.2 Heuristic rules on lane-changing model

The default lane-changing model (Gipps) is used in all the network sections apart from some specific regions that this model results in non realistic merging behavior. In the microscopic model, an on-ramp is followed by an acceleration lane and the drivers entering from the on-ramp need to change lane in order to eventually pass to the mainstream network. In these acceleration lanes, the default lane changing model is replaced with some heuristic rules so as to achieve realistic approaches on the way the drivers merge to the main network from an on-ramp. Additionally, the following heuristic approach is applied to the lane-drop regions giving us more flexibility on reproducing realistic lane-changing decisions throughout the calibration procedure.

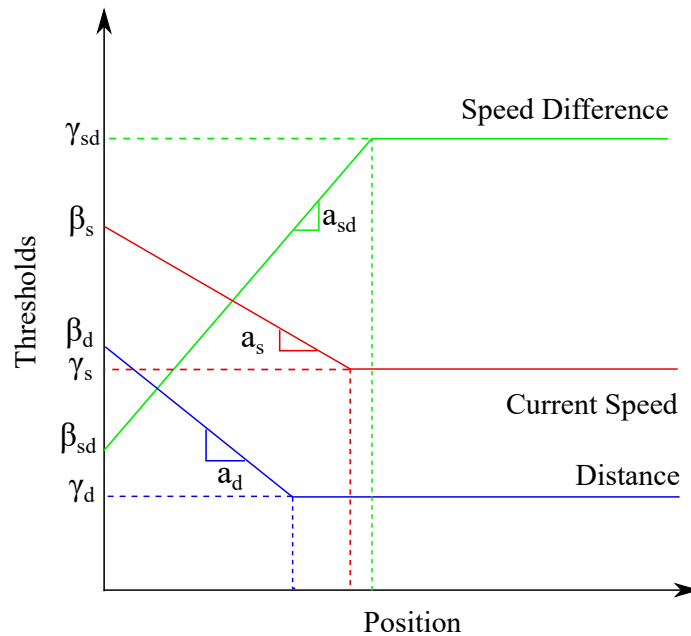


Figure 2.1: Heuristic rules replacing the lane-changing model based on current speed (red line), distance (blue line) and speed difference (green line).

The heuristic rules consist of a set of inequality conditions between the vehicle's current state, and its threshold values. In particular, linear functions of the vehicle's current position determine the threshold values of the three variables of interest i.e. current speed, relative speed with respect to the target-lane vehicles, and available gap in the target lane. The concept of the rules is illustrated in Figure 2.1 where two regimes can be noticed. In the first region the threshold values are linearly dependent on the position of the vehicle while in the second regime the threshold values remain constant. Note that in the first region the current speed and the distance thresholds are decreasing while the threshold of the relative speed difference is increasing with respect to the position of the vehicle. The current state of the vehicle needs to have greater values of current speed and distance than the threshold values of these linear rules while the speed difference has to be lower than the respective threshold value. Once these conditions are simultaneously satisfied then the vehicle is mandated to move to another lane. As it can be observed, the conditions are easier to be satisfied as the vehicle moves further downstream where the threshold values are relaxed.

In order to determine these rules, the required parameters are the slope, the initial and the final value of the linear equations. These parameters are calibrated based on a trial and error process so as to achieve a realistic merging behavior. The calibrated values of the rules are given in Section 4.2.1.

2.3 Calibration and validation processes

The calibration process is the tuning of model parameters to improve its ability to reproduce observed local driver behavior and traffic performance characteristics. Without calibration, the analyst has no assurance that the model will accurately predict traffic state of future scenarios. Validation is the checking process to determine whether the calibration result is suitable to be used on field data (FHWA, 2004). Although the calibration of microscopic models is a tiresome and time-consuming procedure, it is considered as a key part for the reliability of the simulator and the experiments that one can conduct via

these tools.

As it is described in Section 2.1, the calibration studies mainly focus on the adjustment of the parameters used in the separate models of microscopic simulators and not on the adaptation of all the system parameters together. In this case study, there was an initial attempt on manually tuning all the model parameters through a trial and error procedure but due to the high number of degrees of freedom the procedure was labor-intensive. Hence, an optimization algorithm was jointly used in order to find an optimal set of specific parameters that minimize the deviation between the observed and simulated measured speeds. For the purposes of the calibration, a traffic scenario based on the real data of one specific day of the test site network was used while we validated the model with data of some other days.

2.3.1 Calibration process

The calibration procedure that was followed for the purposes of this work consists of several steps. These steps can be categorized as follows:

- **Simulation model**

This step concerns the selection of the test site network and the collection of the necessary data from the field. Afterwards, the network continuously needs to be realistically designed in the microsimulator. The data is used in order to feed the model with the required input parameters and to evaluate the output results of the simulation model. The dynamic scenario is then created where the traffic demand, the turning proportions and some general characteristics like the speed limits and the simulation step are defined.

- **Initial evaluation**

An initial run of the simulation model is conducted with the default parameters of the microsimulator provided by the vendor. This intends to ascertain that there are no notable mistakes on the simulation model as was defined in the previous step

while it gives us the opportunity to decide whether these parameters are sufficient or not. If the simulation output is not satisfactory, we proceed with the calibration.

- **Determination of calibration parameters**

At this point the parameters that have the biggest impact on the network traffic conditions are selected using a sensitivity analysis approach. To this end, the model parameters are modified one by one while keeping the rest constant and the model performance is monitored accordingly.

- **Calibration of parameters**

Once the parameters that effect mostly the performance of the simulation are determined an optimal set of these parameters is searched by coupling the simulation model with an optimization algorithm, aiming at minimizing the difference between the measured speeds and the speeds produced by the simulation model. Note that the heuristic rules that apply in specific sections of the network (see Section 2.2.4) are defined prior to this step so a realistic lane-changing behavior is established. The heuristic rules are further finely tuned in the calibrated model.

- **Evaluation of model's performance**

The calibrated values of the key parameters derived from the optimization problem are set in the micro-simulator. An additional manual tuning on minor parameters is finally conducted.

2.3.1.1 Calibration parameter selection

The parameters used in the models of the microsimulator are categorized into three groups: global parameters, local parameters and particular vehicle type parameters. Global parameters concern all vehicles independent of their type and the section of the network they are driving. On the other hand, local parameters concern the vehicles driving in a particular section of the network while vehicle parameters affect the behavior of the vehicles of a specific type driving anywhere in the network (Transport Simulation Systems, 2014).

Prior to the calibration procedure an initial run is performed using default or best estimates of the simulator parameters and the results are checked for general reasonableness and resemblance to mainline detector station data. In some instances, discrepancies are not caused by the model parameters but rather erroneous demand patterns either in the data collection stage or in the data entry (Hourdakis et al., 2003).

As previously stated, in order to ensure that the simulation performance is close to reality we need to first identify which of the parameters influence most the simulation. Initially, a sensitivity analysis led us to the parameters that have a strong impact in the results of the simulation. These parameters formed the design of an optimization problem that was solved in order to compute their optimal combination.

The most crucial parameters for the simulation performance are:

- Maximum acceleration: This is the maximum acceleration, in m/s^2 , that the vehicle can achieve under any circumstances and is used in the proposed car-following model as the maximum acceleration a .
- Maximum give-way time: When a vehicle has been at a standstill for more than this give-way time (in seconds), it will become more aggressive and it will reduce the acceptance margins. This period is also used in the lane-changing model as the time that a vehicle accepts being at a standstill while waiting for a gap to be created in the desired turning lane before giving up and continuing ahead.
- Normal deceleration: This is the maximum deceleration, in m/s^2 , that the vehicle can use under normal conditions. It is used in the implemented car-following model as the comfortable deceleration variable b .
- Maximum deceleration: This is the most severe braking, in m/s^2 , that a vehicle can apply under special circumstances, such as emergency braking for e.g. in front of a traffic light.
- Minimum Headway: This parameter ensures a minimum time headway between the leader and the follower. Concerning the IDM car-following model it is taken into

account as the desired safety time headway.

- Minimum distance between vehicles: This is the distance, in meters, that a vehicle keeps between itself and the preceding vehicle when stopped. It represents the minimum distance s_o used in the car-following model formulation.
- Maximum desired speed: This is the maximum speed, in km/h , that this type of vehicle can travel at any point in the network. It is also used in the car-following model as the desired speed v_o .

Most of the aforementioned parameters are part of the car-following and lane-changing models employed in our case study microsimulations. The difficulty of the calibration of these parameters yet lies in the fact that these variables are also used in other models that constitute the microsimulator. For instance, the values of the maximum acceleration, the normal and maximum deceleration and the maximum desired speed are essential not only for the calculation of speed but also for the lane-changing decisions, the queue discharge, etc. Likewise, give-way time which is a key aspect of the lane-changing model can also affect the on-ramp capacity in congested situations (Transport Simulation Systems, 2014). Moreover, the substitution of the default behavioral models makes the search of the best-suited parameter sets more tricky considering that the default values of the parameters are not in agreement with the implemented models.

There are other parameters of the microsimulator that affect less the model output but they are relevant to different aspects of the microsimulator. These parameters are manually tuned once the above parameters are defined and are the:

- Reaction time at stop: This is the time it takes for a stopped vehicle to react to the acceleration of the vehicle in front.
- Percentage overtake: This represents the percentage of the speed from which a vehicle decides to overtake.
- Percentage recover: It represents the percentage of the desired speed of a vehicle above which a vehicle may decide to get back into the slower lane.

- Queue Exit Speed: Vehicles that are stopped in a queue whose speed increases above this threshold value are considered to have left the queue and no longer to be at a standstill.
- Queue Entry Speed: Vehicles whose speed decreases below this threshold value (in m/s) are considered to be stopped and consequently, to join a queue.
- Percentage for Staying in overtaking: This parameter defines the percentage of vehicles that stay in a fast lane instead of recover a slower lane during an overtake manoeuvre.
- Percentage for Imprudent lane-changing: This parameter defines the percentage of vehicles that will apply a lane-changing with a non-safe gap.

2.3.1.2 Optimal parameter setting

The key parameters contained in the individual vehicles static attributes are defined by a mean, a maximum and a minimum value. These characteristics for each vehicle are sampled from a truncated normal distribution. In order to obtain an optimal set of values for these parameters, an optimization problem is solved with the aim of minimizing the discrepancies between the observed and the simulation speeds of the network. To this end, a Genetic Algorithm (Goldberg, 1989) is employed in an iterative process.

The Genetic Algorithm Toolbox (MATLAB, 2014) is used in order to solve a constrained optimization problem. The design variables of the optimization problem are the mean values of the selected parameters. The minimum and maximum value of the truncated normal distribution are refined in each iteration based on the current mean values and a constant standard deviation.

The calibration problem is a nonlinear least-squares optimization problem. The objective function concerns the Root Mean Squared Error (RMSE) between the simulated and the actual measured speeds retrieved from detectors across all the lanes of the network. The constraints on the design variables ensure that the calibration values will remain

within natural limits. The optimization problem is formulated as follows:

Minimize:

$$C = \sqrt{\frac{1}{N} \sum_{n=1}^N (V_{sim}^n - V_{real}^n)^2} \quad (2.4)$$

Subject to:

$$L_{\vec{x}_p} < \vec{x}_p < U_{\vec{x}_p} \quad (2.5)$$

where:

C : objective function

V_{sim} : measurements of the simulated speed

V_{real} : real data measurements of the speed

N : number of total observations

\vec{x}_p : model parameter vector

$L_{\vec{x}_p}$: lower limit of simulator parameters \vec{x}_p

$U_{\vec{x}_p}$: upper limit of simulator parameters \vec{x}_p

The genetic algorithm (GA) initializes a population of candidate solutions (hereafter called individuals) and it tries to improve them through a repetitive process. In every iteration, the algorithm applies selection, crossover and mutation operators to the individuals in order to produce new members that replace the old solutions (Holland, 1992). The iterative procedure continues till the objective function (2.4) of at least one individual of the current generation is less than a desirable limit. This individual contains the optimal set of the mean values of the parameters that were earlier discussed.

The optimization cycle is briefly described in Figure 2.2. During each optimization loop, the microsimulation is executed for every individual of the population so that its fitness function can be evaluated. This is achieved by coupling the MATLAB's genetic

algorithm code with the AIMSUN Console. In particular, a Python script serves as an intermediate agent that receives from the GA code the vector of the mean values of one population member and it then passes them to the AIMSUN Console. At this level, the AIMSUN Console is preferred over its Graphical User Interface (GUI) since we need to carry out a vast number of costly simulations. However, we want to ensure that the final set of the calibrated parameters can be also used through the more user-friendly GUI. The input values in the GUI of AIMSUN are though limited to two decimal places. This means that we need to use discrete variables rather than continuous ones in the optimization problem. Therefore, we opt to represent the solution that is contained in each individual of the population with integer values. The Python script then converts the integer parameters to values with two decimal digits by dividing with a proper factor. This way we converted the solution to discrete variables limiting their decimal digits to the maximum number allowed in the GUI, thus making it feasible for other users to input the calibrated values directly in the AIMSUN GUI.

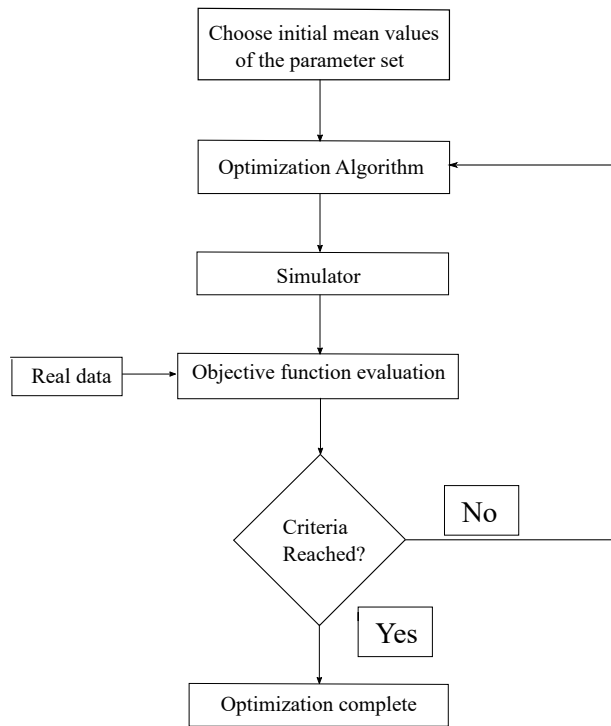


Figure 2.2: Methodology for optimization based model calibration

The integer programming of the genetic algorithm toolbox involves special functions for the crossover and mutation operations (Deep et al., 2009), while for the selection the binary tournament operator is used by default. We finally opted for a population size of 20 individuals which provided a balanced trade-off between computational cost and convergence rate.

2.3.2 Validation process

After the calibration procedure, the resulted model needs to be validated so as to confirm that the microsimulator creates phenomena close to reality under any condition. For that purpose, the microsimulation is performed for the same network but different scenarios are being used that are determined from datasets retrieved from other days. This will ensure that the calibrated model is reliable and the feasibility of the proposed control strategy is subsequently examined based on the assertion that it is applied in a real life network. Once again, the real data speed measurements are used for comparison to the simulation output and specifically the Root Mean Squared Error between the field and the simulation data is evaluated.

Chapter 3

Model predictive control for multilane motorway traffic

3.1 Literature review

In order to overcome the problem of traffic congestion and motorway degradation, numerous traffic management and control methods have been introduced the last decades. It has been envisioned that the deployment of a variety of Vehicle Automation and Communication Systems (VACS) can offer a number of possible advantages on the field of integrated transportation management systems. A number of researchers have proposed innovative traffic control strategies while some of them have considered the possible use of intelligent devices. Some of them are briefly presented below.

Varaiya (1993) proposed the use of intelligent devices in the Automated Highway Systems (AHS), where it was assumed that platoons of fully automated vehicles may travel in specifically designed motorways. This very complex system was suggested to be controlled via a multi-layer control structure, where the traffic flow control strategies are included in a decentralised link-layer.

Hegyi et al. (2005) presented an optimal control problem with the aim of coordinating variable speed limit and ramp metering actions in order to minimize the total time spent in the network. The utilized traffic flow model was METANET (Messner and Papageorgiou, 1990) and a Model Predictive Control (MPC) approach was used in order to solve the

problem. The suggested strategy was tested in motorway traffic networks with the use of only conventional traffic control actuators and vehicles and it was proved that the coordinated use of the control actions could lead to lower time spent in the network.

Kim et al. (2008) took into consideration the possibility of semi-automated or fully automated driving in order to examine lane assignment problems in the AHS. For the lane assignment problem, a partitioned strategy is chosen and the problem is formed as an optimization problem solved with a Genetic Algorithm (GA) with the objective of finding proper positions of partitions.

A hierarchical MPC approach is introduced by Papamichail et al. (2010) considering the use of ramp metering in order to regulate the inflow from an on-ramp to the motorway mainstream. The test site is the Amsterdam ring-road and the outcomes of the application of local feedback control, ideal open-loop control and rolling-horizon hierarchical coordinated control in the field are compared. It was proved that hierarchical control could lead to lower total time spent than the uncoordinated local ramp metering approach in case sufficient ramp storage can be made available.

Baskar et al. (2012) highlighted the benefits of MPC in the AHS. The proposed approach takes into account roadside controllers and intelligent vehicles organized in platoons in the AHS with dynamic speed limits, on-ramp metering and lane allocation used as control measures of the method. For the MPC scheme, a nonlinear and non-convex optimization problem with continuous and integer variables needs to be solved, which is, though, computationally expensive and inconvenient for real-time problems.

Roncoli et al. (2015a) proposed a first-order multi-lane macroscopic traffic flow model for motorways. This traffic flow model stems from the well-known CTM (cell-transmission-model) which is modified and extended in order to include additional aspects of the traffic dynamics such as lane-changing and the capacity drop. In (Roncoli et al., 2015b) this macroscopic model is used for the formulation of a linearly constrained optimal control problem which takes into account the use of VACS both as sensors and as actuators. The convex quadratic problem resulted from the aforementioned formulation is used for the

development of an MPC scheme introduced by Roncoli et al. (2014). The proposed MPC scheme which considers as decision variables, actions that are enabled with the aid of VACS was tested by the use of the AIMSUN microscopic simulator and the results showed that the strategy can lead to amelioration of traffic conditions. Further improvement on the mitigation of congestion was achieved by Roncoli et al. (2016), where a hierarchical MPC framework was developed instead.

3.2 Methodology

Once the calibration results are considered sufficient, a control strategy is applied so as to achieve an improvement of the traffic conditions for the case study network. The proposed strategy is the development of a control framework based on an MPC scheme for the coordinated and integrated motorway traffic management, taking into account the possibility of using VACS both as sensors and as actuators. This leads to the advantages of having an increased degree of freedom with respect to the control possibilities, as well as a more precise estimation of the motorway state, compared to conventional systems.

This control framework is based on a piecewise linear macroscopic traffic flow model with linear constraints which was developed by Roncoli et al. (2015a) while in (Roncoli et al., 2015b) this model with its simple mathematical form is used for an optimal control problem formulation. Additionally, the proposed MPC scheme was tested within the microscopic simulator AIMSUN in (Roncoli et al., 2014), but the case study network at this specific application example was a quite simple network in terms of infrastructure and the microsimulator was set with the default parameters that the software determines. The reader may refer to the aforementioned publications for more details concerning the control framework while for sake of completeness the basic concepts are reproduced below.

Our experiment in the microscopic simulation differs from the previous test case of the proposed scheme in the utilized microscopic network. In this work we study an actual network in the Netherlands with a quite complex infrastructure (on-ramps, off-ramps, lane drop). Furthermore the microscopic simulator in this thesis is initially calibrated and

validated so as to prove that the simulation performance is reliable.

3.2.1 Multi-lane macroscopic traffic flow model

The multi-lane macroscopic traffic flow model described in (Roncoli et al., 2015a) and formulated for the purposes of the optimization problem, stems from the Cell Transmission Model but its simple mathematical form and the further formulation of traffic dynamics aspects makes it an efficient tool for optimal control problem formulations such as the one used in the proposed methodology.

The multi-lane network is subdivided into segment-lane entities with the index $i = 1, \dots, I$ for segments and $j = 1, \dots, J$ for lanes. A discrete time step T for a simulation horizon K indexed by $k = 1, \dots, K$ where the simulation time is $t = kT$. The motorway is discretized in space by defining the segment-lane entities, which are characterized by the following variables:

- Density $\rho_{i,j}(k)[veh/km]$: the number of vehicles in the segment i , lane j , at time step k , divided by the segment length L_i
- Longitudinal flow $q_{i,j}(k)[veh/hour]$: the traffic volume leaving segment i and entering segment $i + 1$ during time interval $(k, k + 1]$, thus remaining in lane j
- Lateral flow $f_{i,j,\bar{j}}(k)[veh/hour]$: the traffic volume moving from lane j to lane \bar{j} (vehicles changing lane remain in the same segment during the current time interval)
- On-ramp flow $r_{i,j}(k)[veh/hour]$: the traffic volume entering from the on-ramp located at segment i , lane j , during the time interval $(k, k + 1]$.

The off-ramp flow is determined according to given turning rates $\gamma_{i,j}$ as a percentage of the total flow passing through all the lanes of the segment:

$$q_{i,j}^{off}(k) = \gamma_{i,j}(k) \sum_{j=1}^J q_{i,j}(k) \quad (3.1)$$

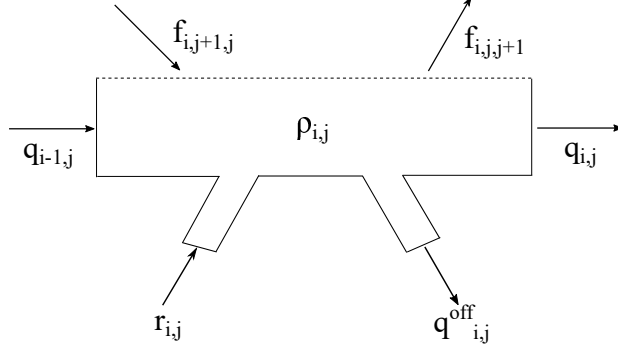


Figure 3.1: The segment-lane variables used in the model formulation

The density $\rho_{i,j}(k)$ is updated based on the following conservation Equation:

$$\begin{aligned} \rho_{i,j}(k+1) = \rho_{i,j}(k) + \frac{T}{L_i} [q_{i-1,j}(k) + r_{i,j}(k) - q_{i,j}(k) - q_{i,j}^{off}(k) + f_{i,j+1,j}(k) \\ + f_{i,j-1,j}(k) - f_{i,j,j-1}(k) - f_{i,j,j+1}(k)] \end{aligned} \quad (3.2)$$

In order to ensure numerical stability of the model, the time step T must respect the Courant-Friedrichs-Lewy (CFL) condition:

$$T \leq \min_{i,j} \frac{L_i}{v_{i,j}^{free}} \quad (3.3)$$

The modeling approach for longitudinal flows is based on a piecewise-linear fundamental diagram (FD) which includes the possibility to reflect the capacity drop phenomenon. As depicted in Figure 3.2, the fundamental diagram consists of the demand part which determines the flow based on the upstream density and the supply part, which determines the flow based on the downstream density. As also mentioned by Roncoli et al. (2015a), the left-hand side of the FD may be modeled via any concave piecewise-linear function, rather than one single line which may lead to more realistic approach of under-critical speed behavior of real traffic flow. Hence this formulation will be used for the purposes of this work.

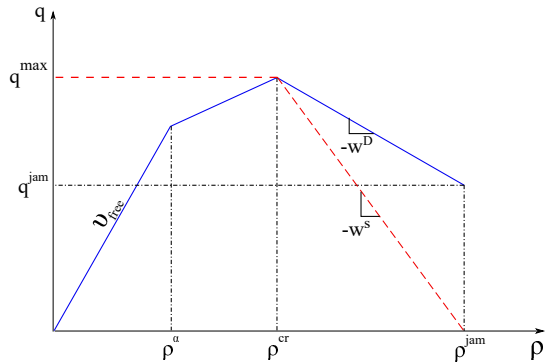


Figure 3.2: The proposed FD including both the demand and the supply piecewise-linear functions.

In the used formulation, the capacity drop is considered supposing that the outflow capacity of a segment-lane is linearly decreasing according to the increase of the current density (in case $\rho_{i,j}(k)$ exceeds the critical density $\rho_{i,j}^{cr}$). This is achieved via the introduction of a linear function that decreases (according to the slope w^D) as the density in the current segment increases. The minimum flow achievable due to the capacity drop is q^{jam} , which occurs when $\rho(k) = \rho^{jam}$. In case no control actions are applied, the actual flow equals the minimum between the demand and supply flows. For optimal control, the longitudinal flows are assumed controllable via corresponding lowering of equipped vehicle speeds as mentioned earlier.

3.2.2 Optimization problem

The previously described multilane traffic flow model, is used for the purposes of an optimal control problem formulation for integrated traffic control under the assumption that a sufficient percentage of vehicles are equipped with VACS, which permits vehicle-to-infrastructure (V2I) communication, to enable variable speed limit control per lane, lane-changing control and ramp metering.

It is assumed that the following control actions are going to be applied for the proposed scheme:

- Ramp metering: these actions consist in regulating the inflow from the on-ramps to the motorway mainstream and since they are applied directly at on-ramps, they do not necessarily require any particular in-vehicle equipment to be performed, as the computed inflow may be directly applied using ordinary traffic signals.
- Mainstream Traffic Flow Control (MTFC) via Variable Speed Limits (VSL): the use of VSL to regulate the mainstream flow with the purpose of mitigating traffic congestion was proposed by Hegyi et al. (2005) and Carlson et al. (2010) and has been exploited in various research works. In the present work, it is assumed that the exiting flows (and consequently, the speeds) are specified for each segment-lane; thus all equipped vehicles travelling on a segment-lane will receive and apply the respective speed or speed limit. For a sufficient penetration of equipped vehicles, this will be sufficient to impose the speed limit to non-equipped vehicles as well.
- Lane-Changing Control (LCC): the optimal lateral flows are computed for each segment-lane, but the implementation of this control action is more challenging and uncertain than the previous two, unless all vehicles are under full guidance by the control centre; in this latter case, it is not difficult to implement the control action by sending lane-changing orders to an appropriate number of vehicles. In all other cases, an intermediate algorithm should decide on the number and IDs of equipped vehicles that should receive a lane-changing advice, taking into account the compliance rate and the spontaneous lane changes; the latter may be reduced by involving additional “keep-lane” advices to other equipped vehicles. Cooperative possibilities of vehicles equipped with V2V-communication capabilities may further facilitate this control action. It is important to highlight that these lateral flows are intended here as macroscopic variables, which does not involve explicitly the characteristics of different drivers, e.g. the origin or the destination of drivers are not considered. This aspect should be accounted for in an intermediate algorithm, that assigns appropriate lane-changing advices to individual vehicles according to their specific needs (e.g., vehicles approaching the desired off-ramp should move towards

external lanes).

In order to guarantee an adequate flexibility, it is supposed that each control action is updated according to a specific control time step which may be specified according to human-factors and other operational requirements. The control time steps are assumed to be integer multiples of the traffic flow model time step. Specifically, we denote by T the model time step, T^Q the MTFC (longitudinal flow control) time step, T^F the lateral (lane-changes) flow control time step, and T^R the RM time step. The corresponding discrete time indices are $k = 0, 1, 2, \dots, K$, $k^Q = \lceil \frac{kT}{T^Q} \rceil$, $k^F = \lceil \frac{kT}{T^F} \rceil$, $k^R = \lceil \frac{kT}{T^R} \rceil$.

Since the main objective of the control strategy is the reduction of traffic congestion, these control actions are taken as decision variables in the formulated optimization problem. In order to make the problem solvable for large networks, it is constructed as a Quadratic Problem (QP), characterized by a convex quadratic cost function and linear constraints.

After the definition of the control steps, the conservation Equation 3.2 for each segment-lane is updated as follows:

$$\begin{aligned} \rho_{i,j}(k+1) = \rho_{i,j}(k) + \frac{T}{L} [q_{i-1,j}(k^Q) + r_{i,j}(k^R) - q_{i,j}(k^Q) - \gamma_{i,j}(k) \sum_{j=1}^J q_{i,j}(k^Q) + \\ + f_{i,j+1,j}(k^F) + f_{i,j-1,j}(k^F) - f_{i,j,j-1}(k^F) - f_{i,j,j+1}(k^F)] \end{aligned} \quad (3.4)$$

Each on-ramp (i,j) receives an *external (uncontrollable) demand* $D_{i,j}[\text{veh}/h]$; since the respective on-ramp outflows $r_{i,j}$ are controllable via corresponding RM actions, this may lead to the creation of *ramp queues* $w_{i,j}[\text{veh}]$. Since the motorway sections and the on-ramps have finite storage capacities, to be imposed as hard constraints in the optimal control problem formulation, excessive external demand scenarios may lead to an infeasible optimization problem, whereby no control action can accommodate the external demands without violating the storage capacity constraints. To avoid such situations, where the admissible control region is void, and enable the computation of optimal control for any

arbitrary demand scenario, we introduce two extra variables: $W_{i,j}[veh]$ that represents a virtual *extra-queue* state variable; and $d_{i,j}[veh/h]$ that represents the demand flow that is *capable to enter into the real queue* $w_{i,j}$ without violating its corresponding upper bound $w_{i,j}^{max}$. The dynamics at on-ramps are thus stated as follows:

$$w_{i,j}(k+1) = w_{i,j}(k) + T[d_{i,j}(k) - r_{i,j}(k^R)] \quad (3.5)$$

$$W_{i,j}(k+1) = W_{i,j}(k) + T[D_{i,j}(k) - d_{i,j}(k)] \quad (3.6)$$

The idea is to apply an extra-strong penalty factor to the variables $W_{i,j}$ so that the solution of the optimization problem is forced to keep the extra-queues equal to zero, if at all possible; but if, due to an excessive demand scenario, there is no other admissible solution, the problem will remain feasible by charging the extra-queues. The longitudinal lane-inflows entering the segment-lanes $(1, j)$ of the first segment are formally treated as on-ramps, however by setting $w_{i,j}^{max} = 0$, they are actually considered uncontrollable. Anyway, also in this case, in order to avoid infeasibility, the same extra-queue approach is applied.

The computation of lateral flows is fully delegated to the optimizer; only upper bounds are specified to the non-negative lateral flows as follows:

$$[f_{i,j,j-1}(k^F) + f_{i,j,j+1}(k^F)] \leq \frac{L_i}{T} \rho_{i,j}(k) \quad (3.7)$$

$$[f_{i,j-1,j}(k^F) + f_{i,j+1,j}(k^F)] \leq \frac{L_i}{T} [\rho_{i,j}^{jam} - \rho_{i,j}(k)] \quad (3.8)$$

$$f_{i,j,j-1}(k^F) \leq f^{max} \quad (3.9)$$

$$f_{i,j,j+1}(k^F) \leq f^{max}$$

Inequality (3.7) represents the upper-bound for lateral flows determined by the number of vehicles in the current lane-segment, Inequality (3.8) is an upper-bound considering the

available space (ρ^{jam} is the maximum admissible density) in the segment-lane that is receiving the lateral flow and Inequalities (3.9) are hard constraints considered in order to strictly limit lateral movements avoiding unrealistic values that cannot be suggested in a real case. Moreover, a cost function term will be introduced in order to discourage lane-changing in dependence of the specific location of each segment-lane.

The lines of the piecewise-linear FD of Figure 3.2 may be simply used as upper bounds for the controllable longitudinal flows as follows:

$$q_{i,j}(k) \leq v_{i,j}^{free} \rho_{i,j}(k) \quad (3.10)$$

$$q_{i,j}(k) \leq \frac{v_{i,j}^{free} \rho_{i,j}^a - q_{i,j}^{max}}{\rho_{i,j}^a - \rho_{i,j}^{cr}} \rho_{i,j}(k) + \frac{q_{i,j}^{max} - v_{i,j}^{free} \rho_{i,j}^{cr}}{\rho_{i,j}^a - \rho_{i,j}^{cr}} \rho_{i,j}^a \quad (3.11)$$

$$q_{i,j}(k) \leq -\frac{q_{i,j}^{max} - q_{i,j}^{jam}}{\rho_{i,j}^{jam} - \rho_{i,j}^{cr}} \rho_{i,j}(k) + \frac{q_{i,j}^{max} \rho_{i,j}^{jam} - q_{i,j}^{jam} \rho_{i,j}^{cr}}{\rho_{i,j}^{jam} - \rho_{i,j}^{cr}} \quad (3.12)$$

$$q_{i,j}(k) \leq v_{i+1,j}^{free} \rho_{i+1,j}^{cr} \quad (3.13)$$

$$q_{i,j}(k) \leq -\frac{v_{i+1,j}^{free} \rho_{i+1,j}^{cr}}{\rho_{i+1,j}^{jam}} \rho_{i+1,j}(k) + \frac{v_{i+1,j}^{free} \rho_{i+1,j}^{cr} \rho_{i+1,j}^{jam}}{\rho_{i+1,j}^{jam} - \rho_{i+1,j}^{cr}} \quad (3.14)$$

Inequalities (3.10), (3.11) and (3.12) represent the demand part of the FD while (3.13) and (3.14) represent the supply part of the proposed fundamental diagram.

The optimization problem is formalized as a convex Quadratic Program (QP), characterized by a convex quadratic cost function and linear constraints, allowing its application also for large networks. The cost criterion to be minimized is defined by the following

Equation:

$$\begin{aligned}
\min_{\substack{\rho, w, W \\ q, r, f}} Z = & T \sum_{k=1}^K \sum_{i=1}^I \sum_{j=1}^J [L_i \rho_{i,j}(k) + w_{i,j}(k)] \\
& + M \sum_{k=1}^K \sum_{i=1}^I \sum_{j=1}^J W_{i,j}(k) \\
& + \sum_{k^F=1}^{K^F} \sum_{i=1}^I \sum_{j=1}^J [\beta_{i,j,j-1} f_{i,j,j-1}(k^F) + \beta_{i,j,j+1} f_{i,j,j+1}(k^F)] \\
& + \lambda^r \sum_{k^R=2}^{K^R} \sum_{i=1}^I \sum_{j=1}^J [r_{i,j}(k^R) - r_{i,j}(k^R - 1)]^2 \\
& + \lambda^f \sum_{k^F=2}^K \sum_{i=1}^I \{ \sum_{j=2}^J [f_{i,j,j-1}(k^F) - f_{i,j,j-1}(k^F - 1)]^2 \\
& + \sum_{j=1}^{J-1} [f_{i,j,j+1}(k^F) - f_{i,j,j+1}(k^F - 1)]^2 \} \\
& + \lambda^{st} \sum_{k=2}^K \sum_{i=1}^I \sum_{j=1}^J \frac{\{q_{i,j}(k^Q) - q_{i,j}(k^Q - 1) + v^{free}[\rho_{i,j}(k) + \rho_{i,j}(k - 1)]\}^2}{(\rho_{i,j}^{cr})^2} \\
& + \lambda^{sl} \sum_{k=1}^K \sum_{i=2}^I \sum_{j=1}^J \frac{\{q_{i,j}(k) - q_{i-1,j}(k) + v^{free}[\rho_{i,j}(k) + \rho_{i-1,j}(k)]\}^2}{(\rho_{i,j}^{cr})^2}
\end{aligned} \tag{3.15}$$

The cost function consists of several terms that we aim to minimize for the purposes of the problem. The first is the Total Time Spent that counts the overall time vehicles spent while travelling in the network and queuing at the on-ramps. The next linear terms aim to penalize the formulation of extra queues and the intense lateral movements during the control strategy. The quadratic terms are introduced in order to penalize time and space oscillations in the control values: ramp outflow, lateral movements, and the speed values; as a matter of fact, the last two terms represent a linearization of the non-linear constraints that consider speed variation; these oscillations are penalized with respect to time and to space.

3.2.3 Control structure

Motorway traffic flow, like most other processes, is affected by several factors, and any related mathematical model has necessarily a limited accuracy. On the other hand, the employed models must be simple enough to allow for computational tractability of the related optimal control problem. For these reasons, the use of an open-loop control strategy (whereby the control trajectories are computed at the initial instant, without being updated during the process) may lead to increasingly diverging process behavior, compared with the predicted one, due to inaccuracies in predicting the external disturbances (mainly the demands) or model mismatches. A mitigation of these issues is offered by the utilization of a receding horizon (or MPC) scheme, that entails that the control actions are re-computed periodically, using updated measurements and predictions. This permits to maintain the difference between the model predictions and the real process outcome at low levels, thus improving the overall control performance.

The control framework, proposed and tested by Roncoli et al. (2014) is composed by three layers and can be schematised as depicted in Figure 3.3.

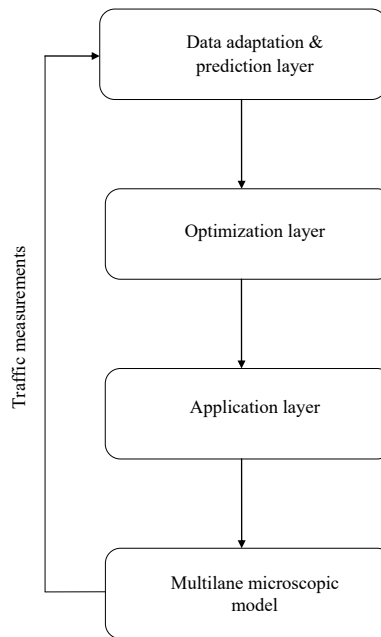


Figure 3.3: Proposed control framework

Each layer can be described as follows:

Adaptation & prediction layer

The purpose of this layer is to essentially process the data retrieved from the motorway system in order to provide necessary information to the lower layers. When conventional vehicles are used, all the data are acquired from traffic sensors placed at specific locations of the motorway (sometimes quite distant from each other). The use of VACS may give the opportunity to extend and enhance the measurement capabilities via available vehicle information from on-board sensors, such as vehicle speed, position (from GPS), and distance to the surrounding vehicles. These data may be shared with other vehicles (V2V communication) or with the infrastructure (V2I communication). These new possibilities lead to an unprecedented accuracy and granularity of available real-time information which opens new avenues for modeling and real-time control.

Traffic demand estimation is a complex task of crucial importance in an MPC framework, since the results of the optimization problem are strongly influenced by a proper forecasting of the expected demand during the defined optimization horizon. Classical forecasting models are based on measurements and historical data elaboration (Burger et al., 2013). Again, a high penetration of VACS may give the possibility of improving the knowledge on the vehicles that are approaching a specific area, permitting to improve the demand prediction accuracy.

Optimization layer

The optimization layer contains the numerical solution of the developed optimization problem, which is solved periodically at predefined control intervals. Since the numerical solution is computed in real-time, a crucial aspect is the time needed to obtain the optimal solution. For the resolution of the optimization problem, the solver Gurobi (Gurobi, 2013) has been utilized, choosing a barrier method algorithm for QP solving. Despite the considerable size of the optimization problem that is obtained even for small networks,

the solution is achieved in a reasonable time.

Application layer

The outcome of the optimization problem needs to be converted to actual control actions present in the motorway system. Specifically, it includes procedures for handling the three defined control actions. The application of RM actions is performed using ordinary traffic signals at on-ramps, via the definition of appropriate green and red phases, which depend on the computed ramp outflows, as detailed in (Papageorgiou and Papamichail, 2008). Alternatively, in presence of VACS, the same results can be obtained providing the commands directly through an in-car information system. These control actions are represented by the control variable $r_{i,j}(k^R)$ and T^R is the control step for RM.

For the MTFC action, the application of speed limits can be improved by the use of VACS. In fact, in the conventional case of manually driven vehicles, the application of a speed limit is effectuated by the use of VMS located on gantries which display the same speed limit for all lanes. The granularity of these actions is also dependent on the distance between successive VMS and cannot be changed. The use of VACS may drastically upgrade the possibilities of applying VSL. In fact, supposing that a sufficiently high number of vehicles is equipped with V2I communication, each equipped vehicle can receive a specific speed limit (or a suggested cruise speed) that should be respected while driving in the current location. In this case, the spatial granularity of the action is completely customizable by the control system, permitting to arbitrarily modify the application areas and lanes without expensive modifications of the infrastructure. A possible further step in this direction could be the integration within Adaptive Cruise Control (ACC) or Cooperative ACC (Vanderwerf et al., 2001), setting the desired speed directly in the vehicle driving systems, without requiring any intervention by the driver. It should be noted that a sufficient penetration of equipped vehicles will be effective to impose the speed limit to non-equipped vehicles as well. Longitudinal flows are defined by the control variables $q_{i,j}(k^Q)$ and T^Q is the control step for MTFC.

The implementation of LCC actions is more cumbersome, even if all vehicles are in communication with the control center. The control actions can be implemented by sending lane-changing advices to an appropriate number of selected vehicles; the selection may be based on the known destinations of the vehicles and further criteria. Since, for a foreseeable future, the lane change advice will not be mandatory, the assignment will have to account for the compliance rate, as well as with other, spontaneous lane-changings decided by the drivers; the latter may be reduced by involving additional “keep-lane” advices to all equipped vehicles that do not receive a lane-change advice. Cooperative lane-changing possibilities of vehicles equipped with V2V communication capabilities may further facilitate the LCC action. Clearly, any mismatch between the optimal lateral flows and the actually triggered lane changes may be partially compensated thanks to the feedback included in the optimization layer.

Chapter 4

Results

4.1 Experimental setup

4.1.1 Test site and data

In the current Chapter, the results of the Model Predictive Control (MPC) strategy are presented. The MPC scheme is applied on a microscopic model that is first calibrated and validated. The calibration was an essential part of this work with respect to the reliability of the models output. The network studied in this work is a stretch of the motorway A20 which is entirely located in the Dutch province South Holland. It links the N213 road of the Westland municipality with the cities of Rotterdam and Gouda, where there at the interchange of Gouwe it connects with the A12 motorway. The case study network concerns only the part of the freeway that connects Rotterdam to Gouda. The necessary data for the input values of the dynamic scenario of the microsimulator and for the evaluation of the models output were taken from (Schakel and Arem, 2014).

of the simulation. Since the calibration of microscopic simulation models depends highly on the completeness and quality of the observed data (Chu et al., 2004), the credibility of the obtained data was initially investigated.

Date	Duration	Long Strech	Sort strech
Monday 26/01/2009	05.00:10.00 AM	~	
Thursday 02/04/2009	05.00:10.00 AM	~	
Tuesday 12/05/2009	05.00:9.00 AM	~	
Monday 08/06/2009	05.00:9.00 AM		~
Thursday 25/06/2009	05.00:9.00 AM		~
Wednesday 26/05/2010	05.00:9.00 AM		~
Monday 21/06/2010	05.37:9.00 AM		~

Table 4.1: Available real data for the test site network

The final implemented network is a stretch of 9.34 km in length and it is composed by three lanes until the 3.6 km where the leftmost lane drops. A deceleration lane appears at 3.4 km which leads to an off-ramp exit at Nieuwerkerk aan den IJssel while 1 km downstream an acceleration lane is encountered that connects the mainstream part of the network with the on-ramp of the same region. At 8 km and 8.5 km there are the deceleration and acceleration lanes for the vehicles exiting and entering from Moordrecht, respectively.

The described network is cautiously designed in the microsimulator while the detectors are placed in the same positions as in reality. This is a crucial task for calibration since our intention is to diminish the deviations between the measured speed from the detectors in the real field and the microsimulation model. There are no detectors measuring the exit and entering flows and speeds in the ramp locations except from one detector placed at the on-ramp Moordrecht. Figure 4.2 illustrates the locations of the detectors in the simulation model.

Detectors locations

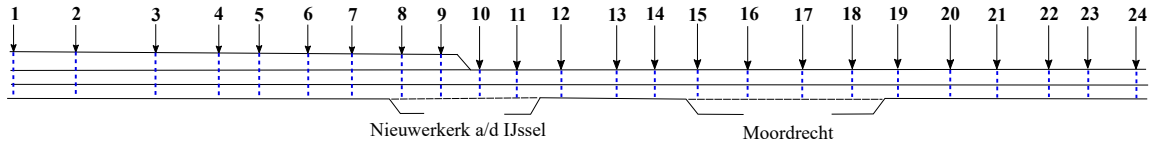


Figure 4.2: Locations of spot detectors placed at each lane of the network

4.1.2 Real traffic conditions

The proximity of the model output to the field data is quantified by exploiting mainly the speed measurements. As a matter of fact, during calibration we aim to set up the simulator so as to produce speeds as close as possible to the real ones. This will lead to the reproduction of real breakdown conditions of bottleneck locations. In order to determine which day's data is going to be used for the calibration procedure, we need to observe the conditions that occur each day and then decide which datasets are the most suitable for our study case.

Figures 4.3 - 4.9 represent the speeds measured from the detectors placed along each lane of the case study network for all the days we have available data. On the right side of each figure the positions of the off-ramps and on-ramps are specified while the dot line in the plot of the speed conditions in lanes 1 and 2 defines the exact location where lane 3 drops. Since lane 3 after some point merges with lane 2 the measured speeds are presented until 3.6 km where the lane drops.

Monday, 26-01-2009, Real Data Speed

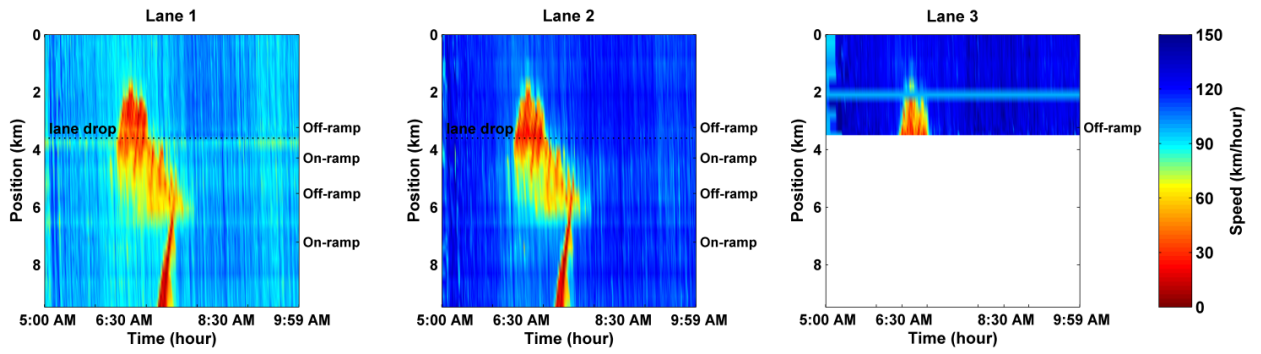


Figure 4.3: Real data speed, Monday 26-01-2009

Thursday, 02-04-2009, Real Data Speed

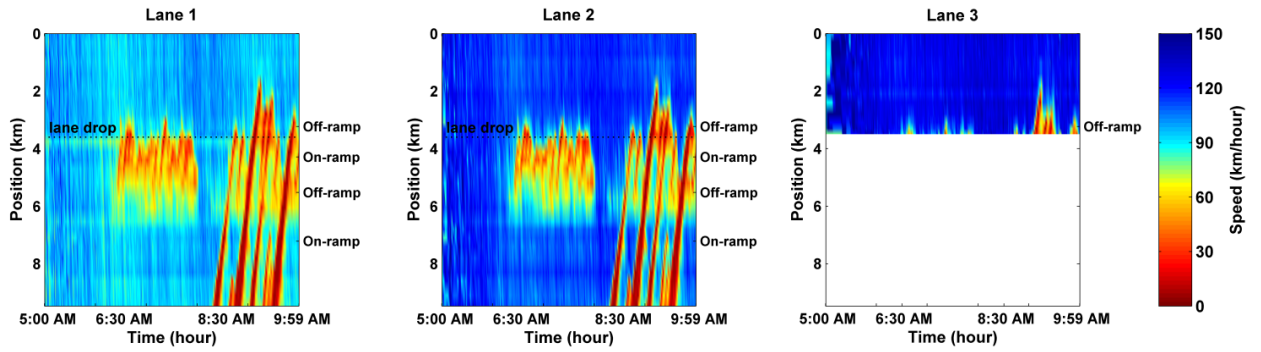


Figure 4.4: Real data speed, Thursday 02-04-2009

Tuesday, 12-05-2009, Real Data Speed

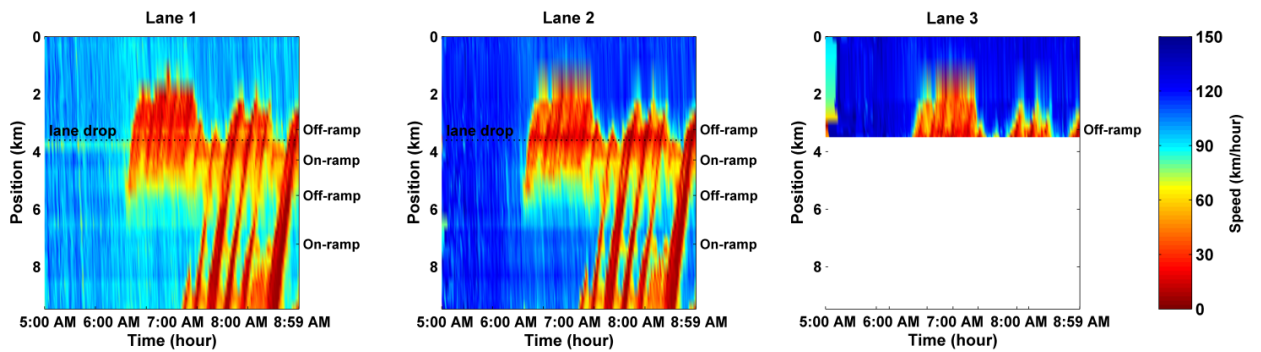


Figure 4.5: Real data speed, Tuesday 12-05-2009

Monday, 08-06-2009, Real Data Speed

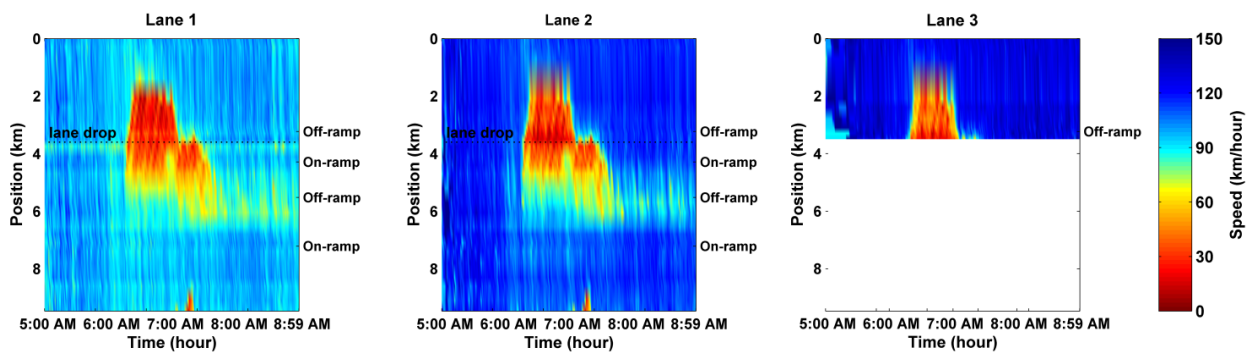


Figure 4.6: Real data speed, Monday 08-06-2009

Thursday, 25-06-2009, Real Data Speed

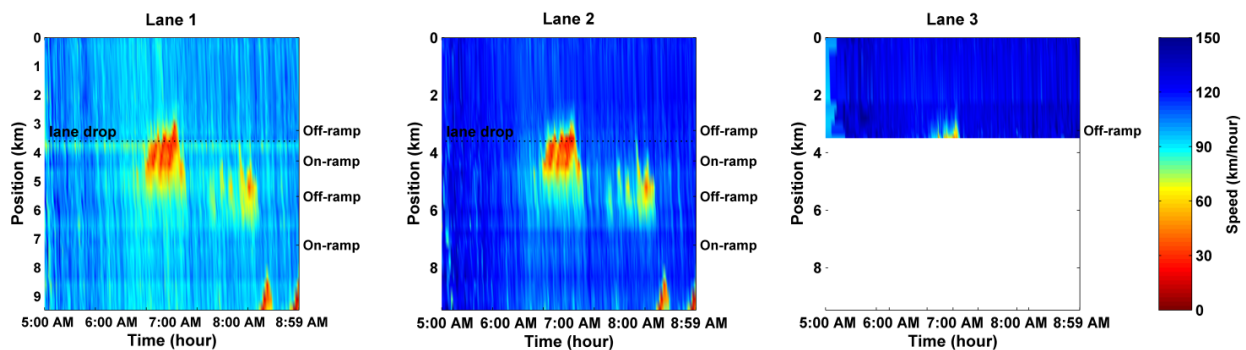


Figure 4.7: Real data speed, Thursday 25-06-2009

Wednesday, 26-05-2010, Real Data Speed

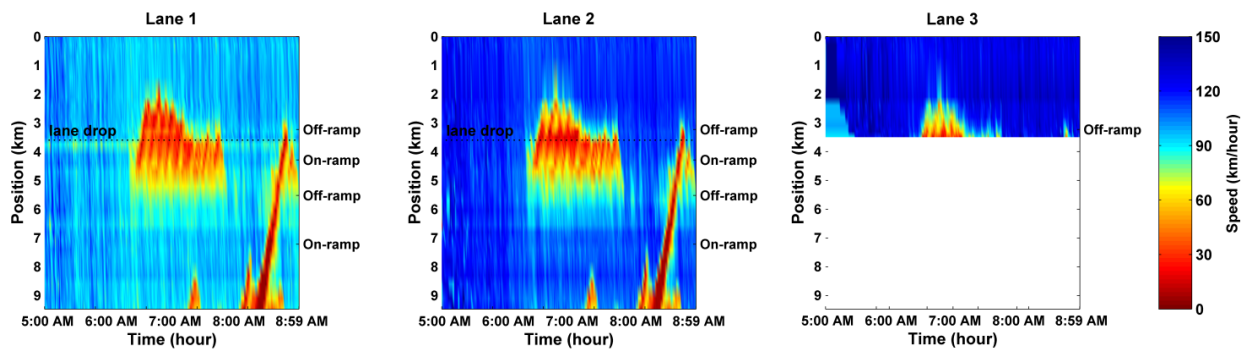


Figure 4.8: Real data speed, Wednesday 26-05-2010

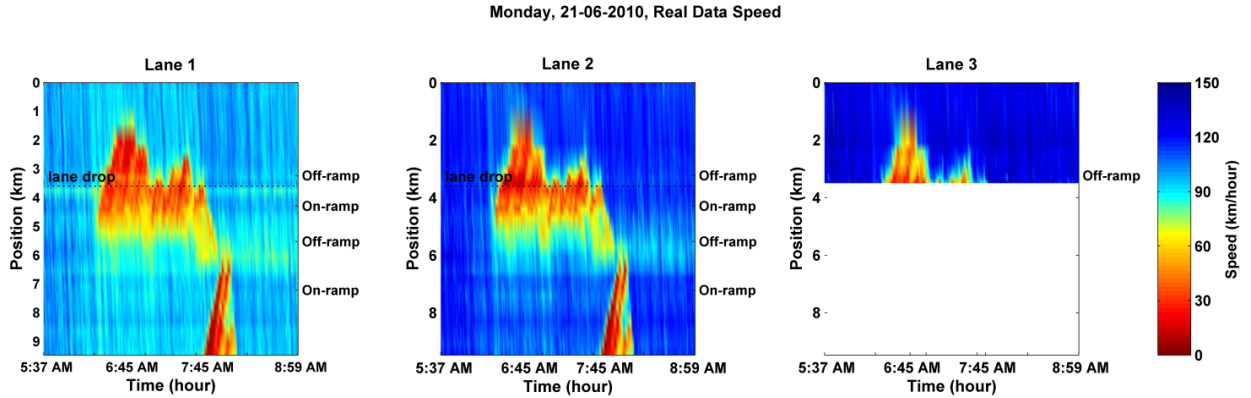


Figure 4.9: Real data speed, Monday 21-06-2010

The congestion pattern of the network can be extracted from the speed measurements demonstrated in the above figures for each day:

- **Monday, 26-01-2009:** Congestion is initiated at around 06:30 AM and lasts until 8:00 AM. A bottleneck appears at the location of off-ramp Moordrecht and spills back upstream where standing queues are created due to the lane-drop. At around 07:30 AM there is also a moving jam from the downstream end of the section.
- **Thursday 02-04-2009:** At this day two different bottlenecks occur throughout the five hour period considered. The first appears from 6:30 AM until 8:00 AM and stems from off-ramp Moordrecht while the second lasts from 09:00 until the end of the the measurement period and is triggered from congestion created at the end of the network.
- **Tuesday 12-05-2009:** The speed contour plot of this day illustrates similar traffic conditions to the ones of “Thursday 02-04-2009” with the difference that the congestion emerging this day is quite stronger. The two bottlenecks interfere with each other and this results to a longer duration of the congestion from 06:30 AM until around 09:00 AM.

- **Monday 08-06-2009:** The congestion pattern for this day is quite clear. The main source of the traffic jam is the increased demand from on-ramp Nieuwerkerk aan den IJssel and the congestion is extended further upstream where there are also queues formed due to the lane drop. A small moving jam spills back from the exit of the freeway at 07:00 AM.
- **Thursday 25-06-2009:** The congestion arising this day is pretty mild and is activated again due to the high flow entering from on-ramp Nieuwerkerk aan den IJssel from 07:00 AM to 07:30 AM while a small reduction on the speed appears also at around 08:00 AM due to off-ramp Moordrecht.
- **Wednesday 26-05-2010:** The traffic pattern of this day consists of a bottleneck starting at the on-ramp Nieuwerkerk aan den IJssel and propagating upstream where there are also queues created due to the lane drop. The congestion lasts from 06:30 AM until 07:30 AM and some small traffic jams that propagate upstream from the exit of the network (A12) are also appearing.
- **Monday 21-06-2010:** The traffic conditions in this day are quite similar to the one above. The increased demand entering from on-ramp Nieuwerkerk aan den IJssel combined with the deterioration of traffic conditions due to the lane drop are the main sources of congestion. Some mild congestion appears at the exit of the network.

Note that concerning the traffic jams originated at the exit of the network and the related spilling back, no boundary conditions are going to be set in order to replicate such phenomena in the microscopic model. In addition to this, the fact that calibration process will be ensued by the application of a model predictive control strategy will play a key role to the selection of the real dataset to be used in the calibration. The control actions that will be imposed during the MPC scheme concern lane-changing cooperation, variable speed limits and ramp metering. Based on the above rationale, the datasets that can be used for the model's calibration are eliminated to the following:

- Monday, 08-06-2009
- Thursday, 25-06-2009
- Wednesday, 26-05-2010
- Monday, 21-06-2010

Eventually, the parameters of the simulation model will be tuned in order to replicate traffic conditions of “Wednesday 26-05-2010”. The dynamic scenario is determined based on the traffic flow measurements of this day while the observed speeds will be used in order to evaluate the model’s performance. Similarly, the datasets of the rest days will be used in order to validate the model.

4.1.3 Dynamic scenario

The dynamic scenario contains the necessary input data and experiments to execute one or several processes. A scenario consists of several parameters with the most significant being the traffic demand while additional inputs could be public or master control plans. In the dynamic scenario the AIMSUN API file is also defined which is utilized for the communication between the user and the simulator in real-time simulation.

In order to create the traffic demand of the simulation’s scenario, we need to first identify the vehicle types to be used. The field data does not have any distinction between different vehicle types so we consider that the simulated flow concern only conventional cars. Consequently, we construct the traffic states for this single vehicle type and for one minute time interval same as the real data measurement interval. The traffic states will compose the traffic demand which is assigned in the scenario. Since the available data for the model calibration durates from 5:00 AM to 9:00 AM, 240 traffic states are created and a four hour simulation scenario is developed.

Each traffic state describes the state in each section of the network and the time interval we have prescribed. The traffic states are characterized by the input flows in sections that act as vehicle entries to the network and by turning percentages for the rest

sections and turns. In our case study, we need to define the entering flow at each lane of the mainstream and also at the two on-ramps. Since there are no available detector data at on-ramp locations, the flow at these entrances is computed based on the measurements of the flow from the detectors placed before and after the locations that vehicles enter the mainstream network from the on-ramps. Similarly to this, due to the lack of data at off-ramp locations the percentage of vehicles exiting the network via an off-ramp is again calculated based on the flow measured before and after the off-ramp.

4.2 Calibration and validation

4.2.1 Parameter setup

In the first stage of the calibration we adjusted some general parameters of the model. These parameters are the simulation step $T = 0.4$ sec and the speed limit in each section which is set equal to 120 km/h. Consequently, the optimal values of the parameters with a significant influence on the performance of the vehicles in the network were found based on the solution of the optimization problem described in Section 2.3. The values of these parameters are listed below in Table 4.2.

Parameter	Mean value	Deviation	Min Value	Max Value
Max acceleration (m/s^2)	2.46	0.2	1.87	3.07
Normal deceleration (m/s^2)	2.81	0.2	2.21	3.41
Time Headway (sec)	0.88	0.1	0.58	1.18
Min distance vehicle (m)	2.83	0.3	1.93	3.73
Max Desired Speed ($km/hour$)	120	14.8	80	150
Maximum Give-Way time (sec)	12.97	2.64	7.69	18.25

Table 4.2: Mean, deviation, minimum and maximum values of calibrated key parameters

Although the microscopic simulation model with the use of the values demonstrated in Table 4.2, can reflect general aspects of the actual traffic conditions, it lacks in reproducing some features. For instance, the microsimulation can capture the initial time and location of congestion but it is unable to replicate the duration and the upstream propagation length of traffic jams. Moreover, the vehicle distribution among the different lanes appears to be not well-predicted. The latter conditions, though, are eventually fulfilled by manually calibrating the rest of the parameters that were not included in the optimization problem and by improving the heuristic rules determining the lane-changing behavior in specific sections. The final values of the manually calibrated parameters are given in Table 4.3 while the applied heuristic rules are subsequently described.

Parameter	Calibrated Value
Reaction time at stop (<i>sec</i>)	0.7
Percentage Overtake (%)	93
Percentage Recover (%)	94
Queue Entry Speed (<i>m/s</i>)	2
Queue Exit Speed (<i>m/s</i>)	5
Percentage for staying in overtaking (%)	10
Percentage for Imprudent lane-changing (%)	40

Table 4.3: Values of manually calibrated parameters

The heuristic rules described in Section 2.2.4 replace the default lane-changing model in merge areas where the Gipps model results in problematic merging situations. These regions are the acceleration lanes after the two on-ramps and the lane drop. Vehicles driving in the acceleration lanes need to eventually move to the adjacent lane so as to enter the mainstream before that lane drops. The decision for that lane change depends on

its current position and speed, the relative speed with respect to the mainstream vehicles and the available gap in the mainstream. The aforesaid variables are compared to the respective threshold values and in case all the conditions are satisfied the vehicle changes lane. Numerous tests for the identification of the most appropriate threshold values were conducted while Figure 4.10 illustrates the applied rules in the acceleration lanes.

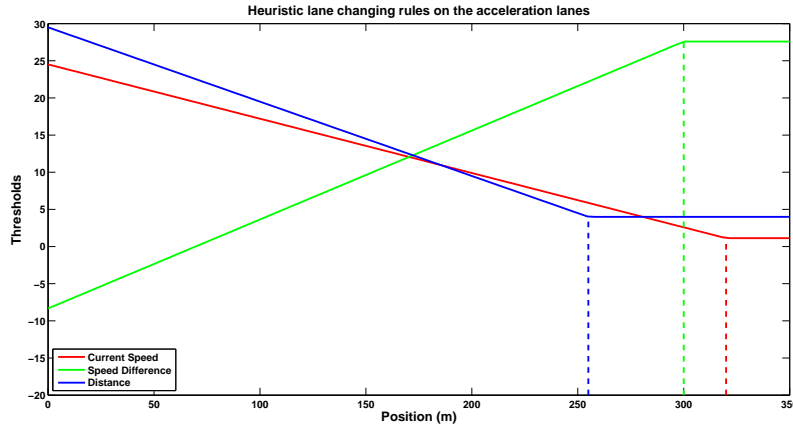


Figure 4.10: Heuristic lane-changing rules applied in the acceleration lane

The calibration of these rules in the section with the lane drop was quite tricky considering that in reality there are bottlenecks created due to the queues formed in that location. Hence, we had to tune the criteria parameters so as to achieve on the one hand realistic merging behaviors and on the other hand manage to create the standing queues at the merge point. The chosen values of the heuristic rules in the lane-drop region are shown in Figure 4.11.

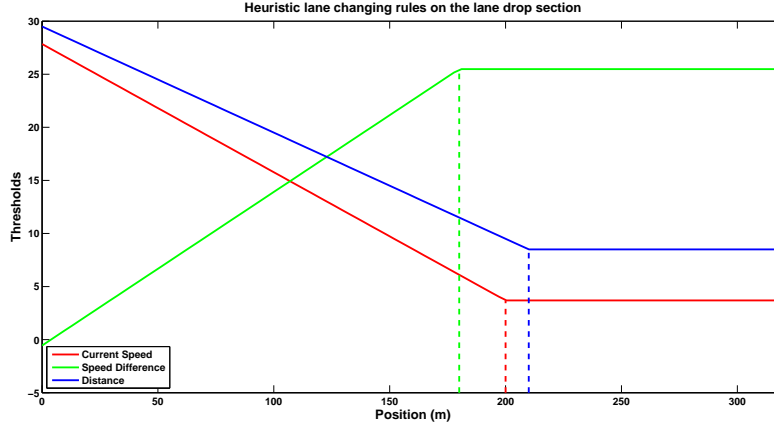


Figure 4.11: Heuristic lane-changing rules applied in the lane drop

It can be observed that based on these rules the vehicles driving in the aforementioned regions are getting more aggressive while they are approaching the merging points in both cases.

4.2.2 Calibration results

Throughout the calibration procedure, the error between the simulated and the observed speed is the index to be minimized (Equation 2.4). The traffic conditions produced by the calibrated model are illustrated in Figure 4.13 while for the sake of completeness the real data speed is shown again in Figure 4.12.

Congestion is created due to the increased demand at on-ramp Nieuwerkerk aan den IJssel at the same time as in the real life network. The duration and the locations that bottlenecks appear are in very good agreement with reality. The traffic jams spilling back from the exit of the network in the observed data are not reproduced in the simulation model since no boundary conditions are set. The Root Mean Squared error between the simulated and field speeds is $RMSE = 19$ km/hour.

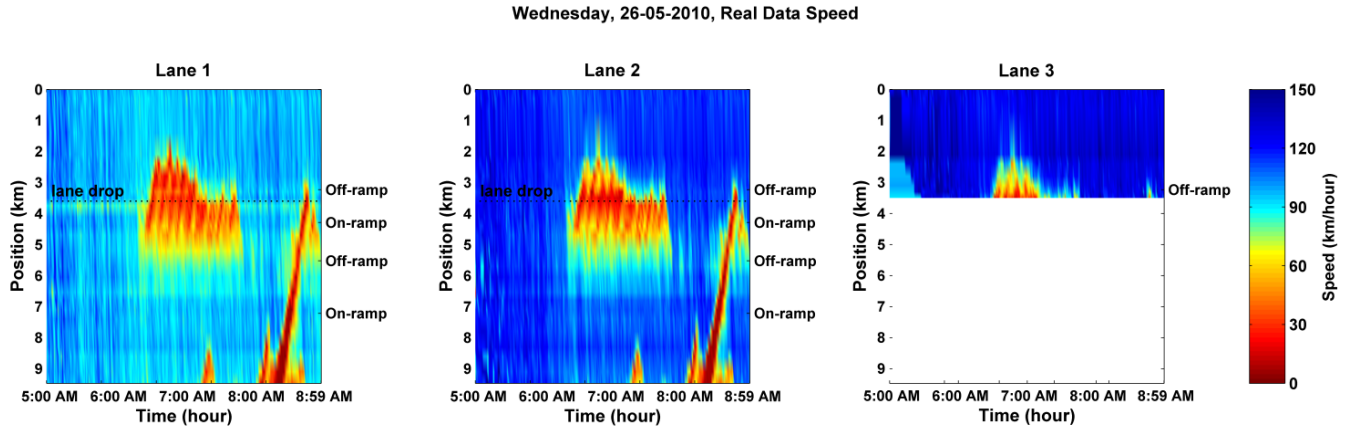


Figure 4.12: Real data speed, Wednesday 26-05-2010

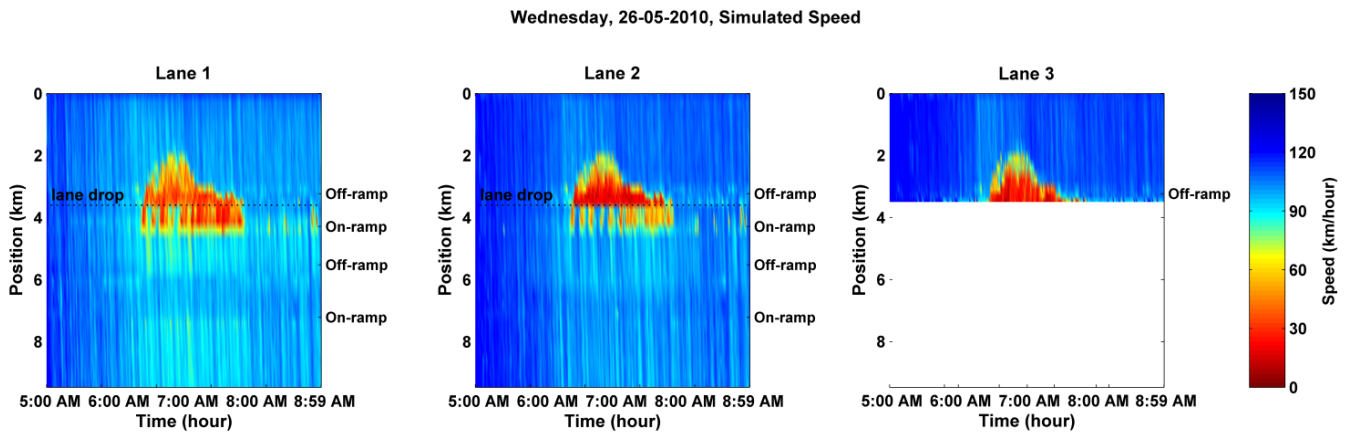


Figure 4.13: Simulated speed, Wednesday 26-05-2010

The detector locations were previously demonstrated in Figure 4.2 and below the aggregated flows measured at each one of these locations are presented at Figures 4.14 - 4.19. The red color line illustrates the measured flows in the microscopic model while the blue line color concerns the real data traffic flows. Except from some minor portions of the network, the simulated flow is strikingly similar to the real flow measurements. Most importantly, it is apparent that the calibrated model is capable of reproducing the capacity drop phenomena. This drop of the outflow firstly appears at “Detector location

12” (Figure 4.16) which is after the on-ramp Nieuwerkerk aan den IJssel where congestion is triggered.

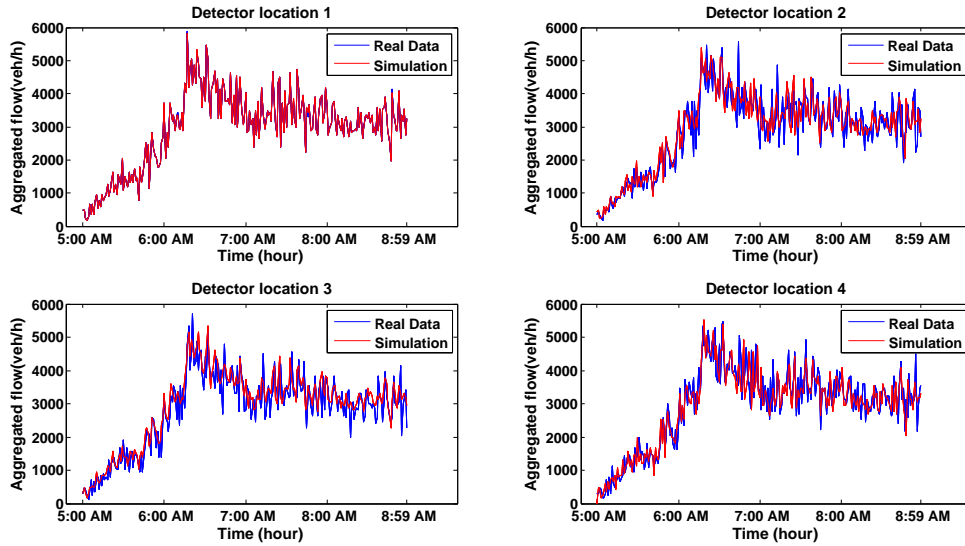


Figure 4.14: Comparison between measured (blue line) and simulated (red line) aggregate flow at detector locations 1-4

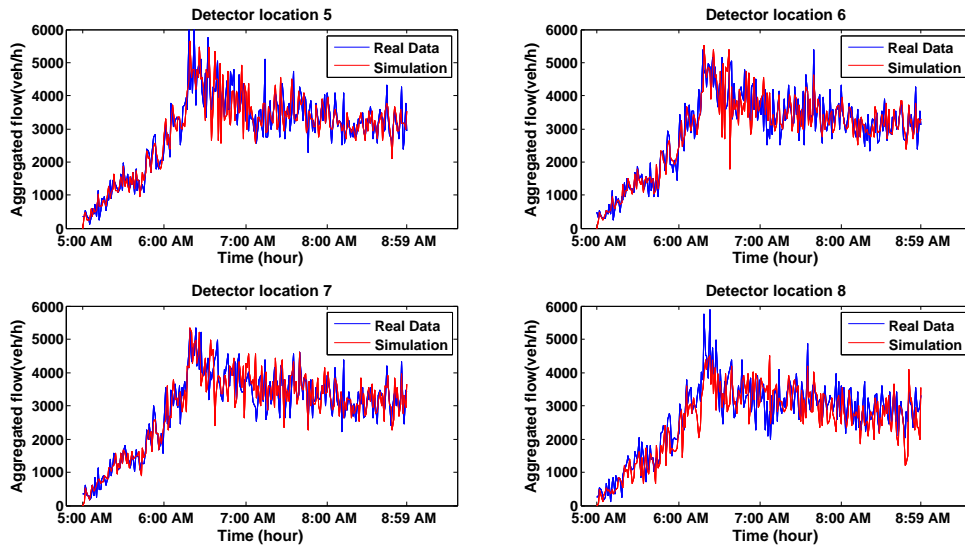


Figure 4.15: Comparison between measured (blue line) and simulated (red line) aggregate flow at detector locations 5-8

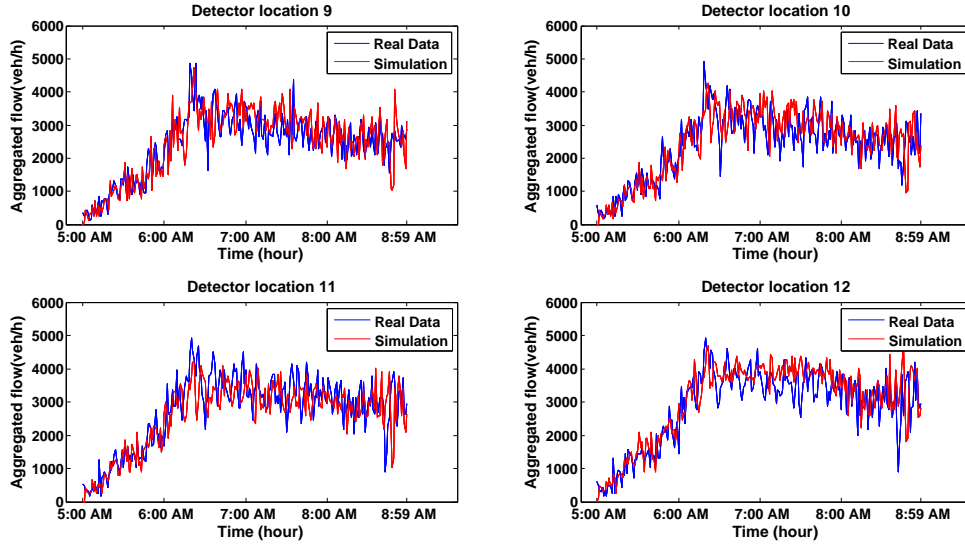


Figure 4.16: Comparison between measured (blue line) and simulated (red line) aggregate flow at detector locations 9-12

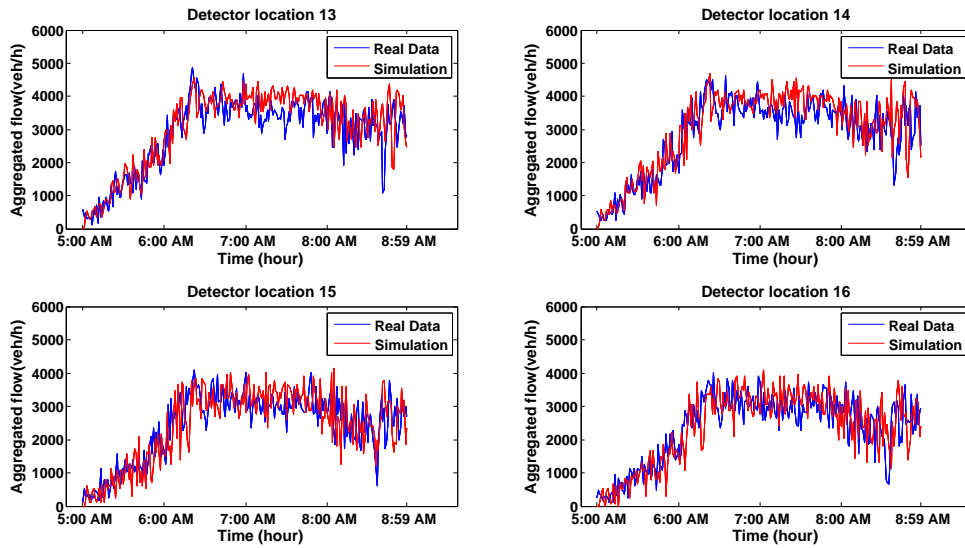


Figure 4.17: Comparison between measured (blue line) and simulated (red line) aggregate flow at detector locations 13-16

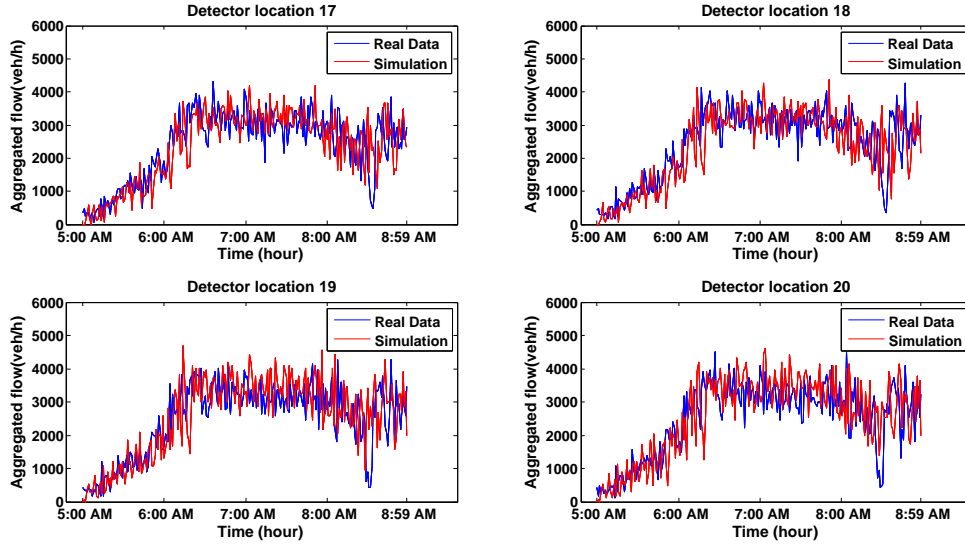


Figure 4.18: Comparison between measured (blue line) and simulated (red line) aggregate flow at detector locations 17-20

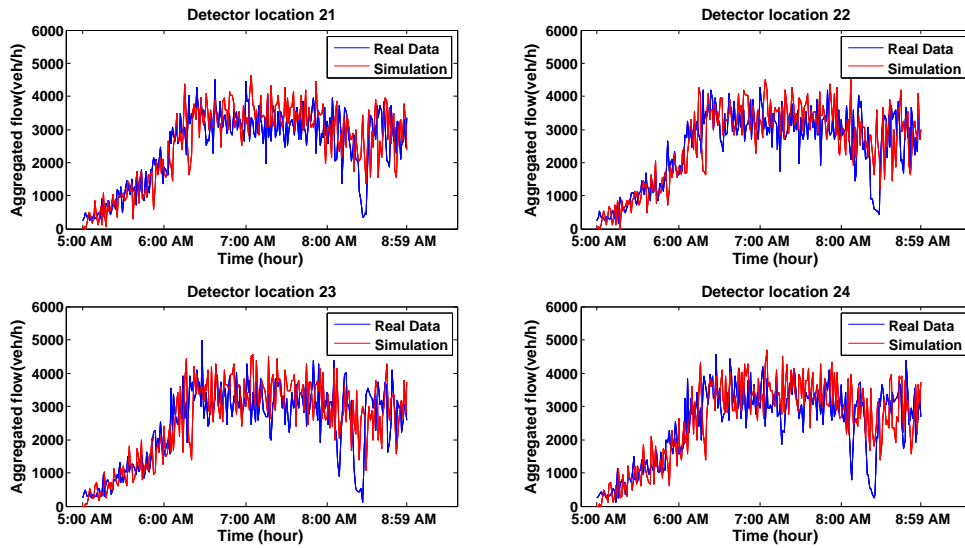


Figure 4.19: Comparison between measured (blue line) and simulated (red line) aggregate flow at detector locations 21-24

4.2.3 Validation results

The purpose of validation is to confirm that the calibrated model can replicate real life traffic scenarios under other conditions as well. To this end, different demand profiles are set in the dynamic scenario based on the field data collected on different days. The performance measure for the validation is again the speed measured across the network while the Root Mean Squared Error between the real and the simulated speeds is computed. Below, the traffic pattern produced by the calibrated model is compared to the real traffic conditions of each one of the selected days.

- **Monday 08-06-2009:** The traffic conditions produced by the simulator, approach reality quite well. The congestion is activated due to entering flow from on-ramp Nieuwerkerk aan den IJssel and it propagates upstream covering the same length of the network in both cases. The duration of the bottleneck is quite different since in the simulation model it lasts about half an hour less. Moreover congestion should be eliminated upstream the lane-drop location after 07:00 AM but in the simulation output we observe that it lasts more. The root mean squared error between the simulated and the field speeds on this day is $RMSE = 17$ km/hour.

Monday, 08-06-2009, Real Data Speed

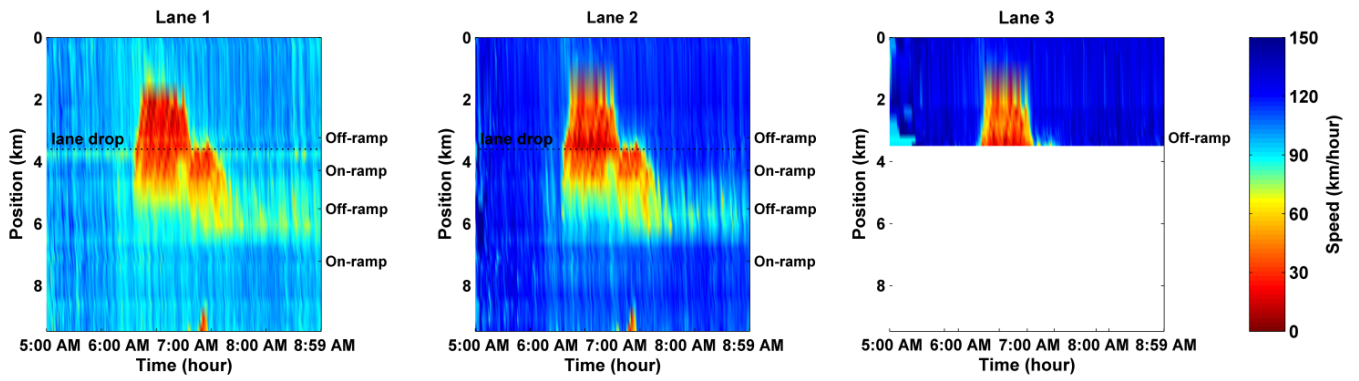


Figure 4.20: Real data speed, Monday 08-06-2009

Monday, 08-06-2009, Simulated Speed

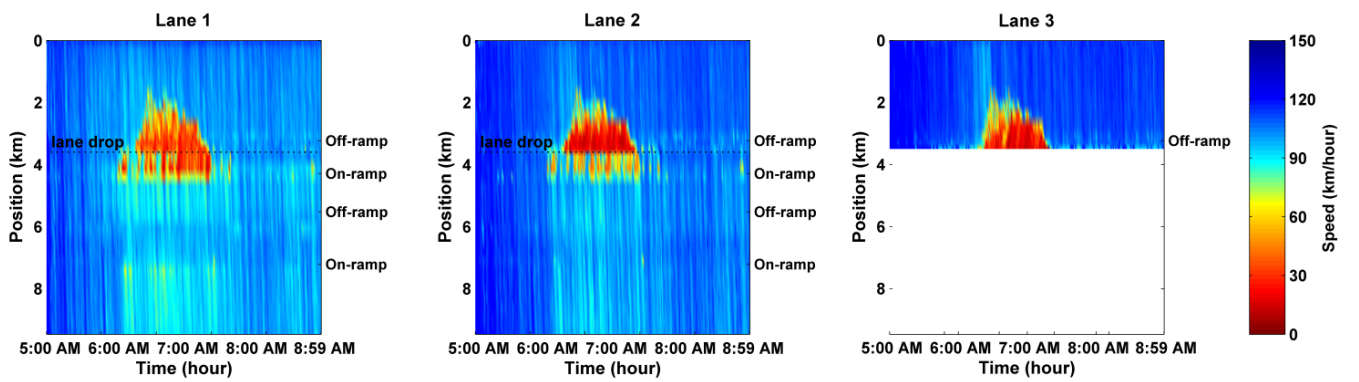


Figure 4.21: Simulation speed, Monday 08-06-2009

- Thursday 25-06-2009:** Congestion in the simulation model appears to be rather mild compared to speed measured from the field while the small traffic jam due to off-ramp Moordrecht is not reproduced. Apart from that, the main bottleneck is created due to the increased demand in Nieuwerkerk aan den IJssel on-ramp at 06:30 AM and lasts until 07:00 AM in both cases while the root mean squared error between the model and the field speed is $RMSE = 22.5$ km/hour.

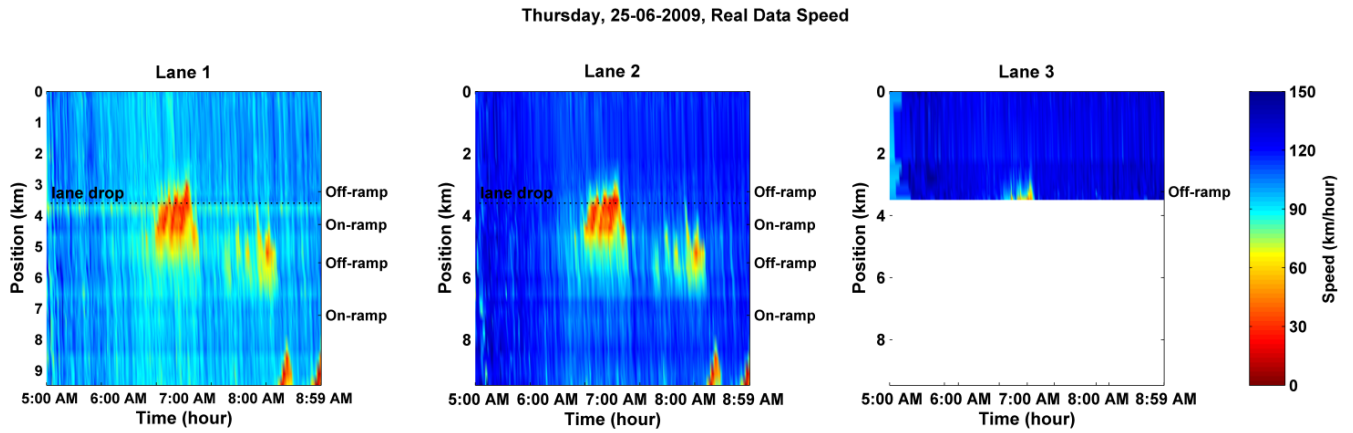


Figure 4.22: Real data speed, Thursday 25-06-2009

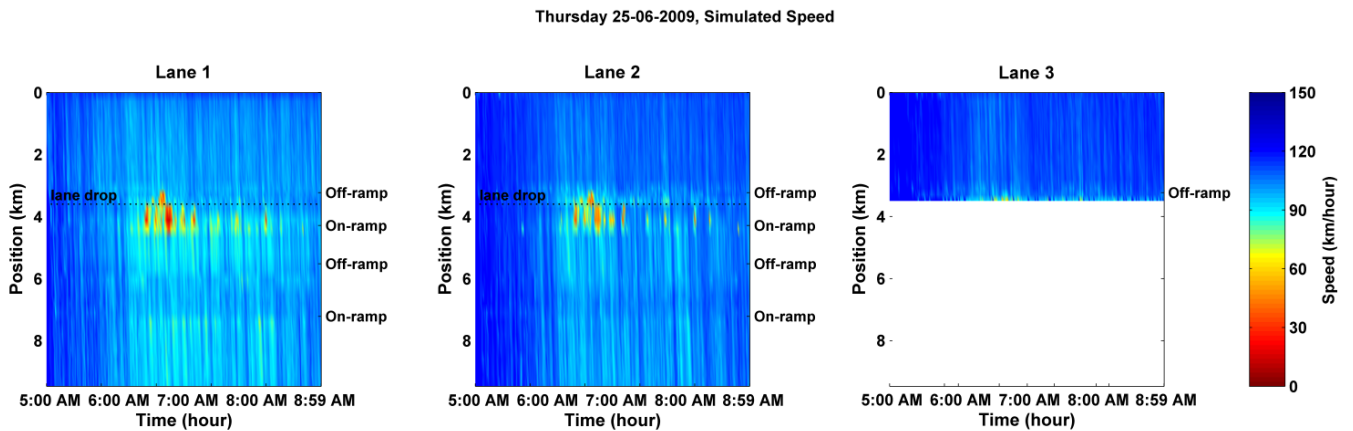


Figure 4.23: Simulated speed, Thursday 25-06-2009

- Monday 21-06-2009:** The calibrated model sufficiently replicates the traffic conditions of this day. The initial location, time and duration of congestion in the simulation model matches well with the real data. However there are discrepancies between the model and the field measured speeds since it seems that the created congestion in the simulation model is quite stronger than the one in reality. The computed error between the simulated and the observed speed is $RMSE = 21$ km/hour.

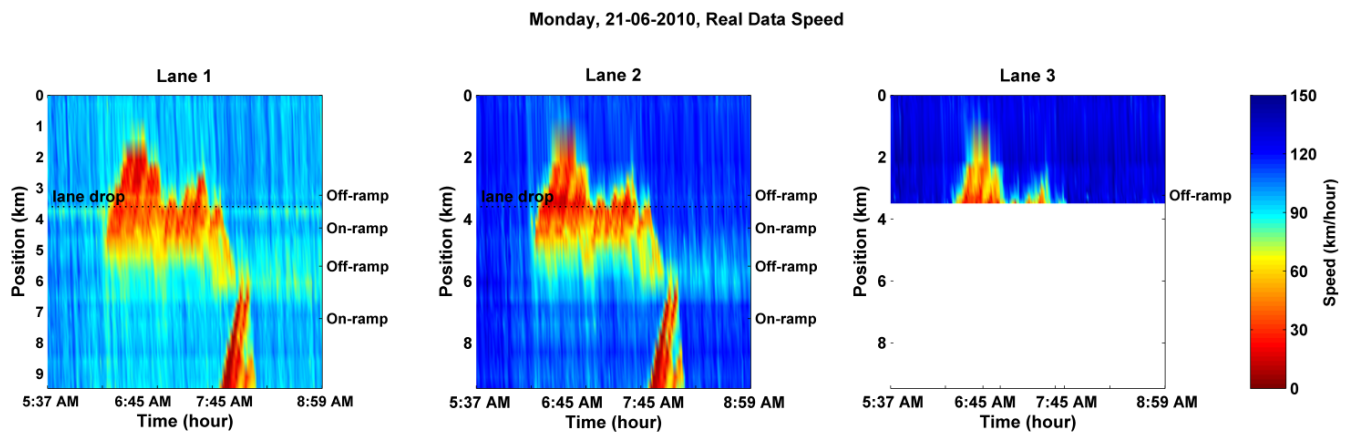


Figure 4.24: Real data speed, Monday 21-06-2010

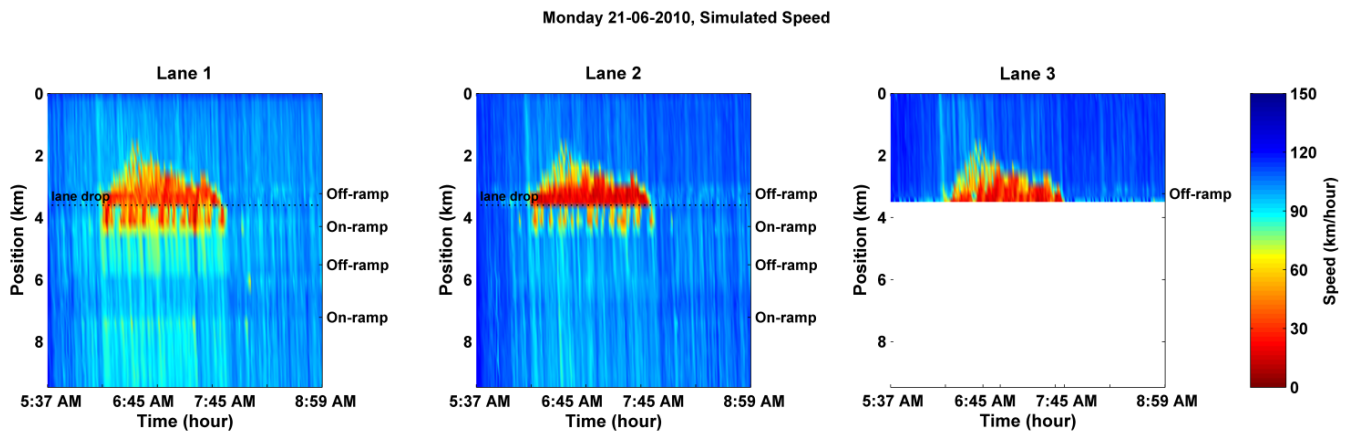


Figure 4.25: Simulation speed, Monday 21-06-2010

4.3 Application of model predictive control

4.3.1 Optimization problem setup

The calibrated multilane model will be used in order to test the feasibility and the effectiveness of the MPC strategy (Section 3.2) under realistic traffic conditions. The network, which as described before has about 9.3 km length, is subdivided in 21 segments with the length of each segment indicated in Figure 4.26. It is composed by 3 lanes until segment 8 where we have the drop of lane 3 and successively there are two lanes. In segment 8 there is the first off-ramp leading to Nieuwerkerk aan den IJssel while in segment 10 there is the on-ramp for vehicles entering the freeway from Nieuwerkerk aan den IJssel. In segments 14 and 16 the off-ramp and on-ramp for vehicles exiting or entering from Moordrecht are encountered.

The same dynamic scenario will be used as the one in the calibrated model with the accommodation of an additional control plan for the RM actions. The control plan lasts from 5:00 AM to 9:00 AM similarly to the duration of the simulation. Traffic lights are placed 10 m upstream of the merging point between the on-ramps and the acceleration lanes that lead to the freeway.

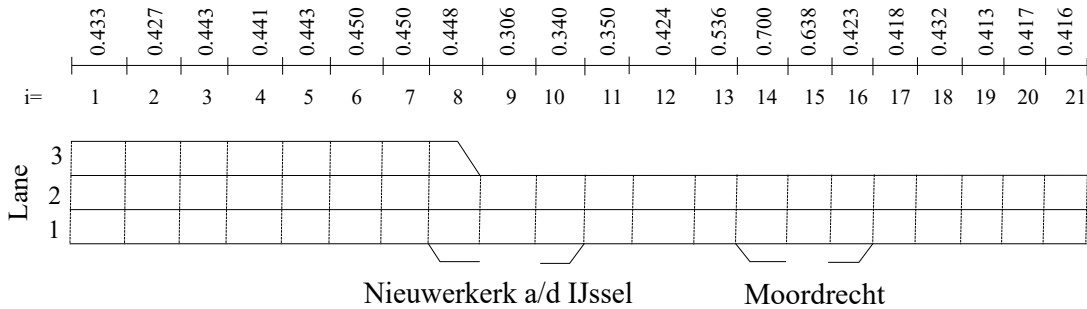


Figure 4.26: Schematic representation of the case study network discretized in 21 segments

Regarding the macroscopic traffic flow model of the optimization problem that is described in Section 3.2, the simulation step is set to $T=10$ sec which is the maximum value that satisfies the CFL stability condition. Once the simulation step is chosen, the

control steps for RM and LCC are set to 1 min while for MTFC we choose a time step equal to the simulation step since, within the optimization problem, the longitudinal flows are constrained by linear functions that depend on the current densities (which in turn are updated according to the simulation step). Hence, in case the control step includes more than one simulation step, there is only one active constraint (the one considering the minimum density) that causes to unnecessarily bound the longitudinal flows also for simulation intervals when density is actually higher (Roncoli et al., 2014). For the optimization problem a horizon time of 10 minutes is selected and the update period is taken to be 1 minute. The demand during the optimization horizon is a constant value set equal to the exponential smoothed value of the past demand.

The cost function to be minimized (Equation 3.15) in the optimization problem is composed by various terms with weights that need to be specified based on the characteristics of our problem. In the following Tables (4.4-4.6) the coefficient values that were used in this study are demonstrated. These coefficients were kept constant throughout the simulation.

The weight parameters of the quadratic terms have been tuned and the values of Table 4.4 are used in our case study.

M	λ_f	λ_r	λ_{st}	λ_{sl}
10	10^{-8}	10^{-8}	10^{-6}	10^{-7}

Table 4.4: Weight parameters of the quadratic terms

In order to exclude the possibility of vast number of lateral movement which may lead to deterioration of the traffic conditions a penalty coefficient need to be set. On the other hand in specific locations where strong lateral movement is expected the relevant penalty coefficient should be set lower. Such locations are sections upstream the lane-drop and the on-ramps and downstream the off-ramps. The value of the weight $\beta_{i,j,\bar{j}}$ is set in all the segments $\beta_{i,j,\bar{j}} = 0$ except from the segments-lane entities specified in Tables 4.5.

Segment\ Lane	6	7	8
2	10^{-6}	10^{-6}	10^{-3}
3	10^{-8}	10^{-8}	10^{-3}

Segment\ Lane	9	15
1	10^{-6}	10^{-3}
2	10^{-8}	10^{-8}

Table 4.5: Coefficient for right and left lateral movement

The upper bounds for the maximum flow allowed to enter and exit from on-ramps and off-ramps are specified. Additionally, maximum values of lateral movements and of on-ramp queues are determined and presented in the Table 4.6.

Bounds					
$w_{10,1}^{max}$ [veh]	$w_{16,1}^{max}$ [veh]	r^{min} [veh/hour]	r^{max} [veh/hour]	r_{off}^{max} [veh/hour]	f^{max} [veh/hour]
20	30	120	3000	3000	1000

Table 4.6: Values of upper and lower bounds

The model formulation for longitudinal flows is based on a piecewise linear fundamental diagram with the demand and the supply part of the FD determining the flow based on the upstream and the downstream density, respectively. The left-hand side of the FD consists of two lines in order to achieve more realistic speed behavior in case of undercritical densities. The proposed traffic flow model allows the introduction of different parameter values of the fundamental diagram for each segment-lane entity. Although in our case study network the traffic conditions of each link lead to quite different fundamental diagrams, such a discretization would lead to numerous parameters to be defined and most probably to over-parametrization. Accordingly, the use of only two different FDs is decided, one for segment 8-lane 2 and one for the rest part of the network. This choice was made due to the fact that lane 3 in segment 8 drops and merges with lane 2, and a strong lateral movement is expected from lane 3 to lane 2 as a result of it. These intense lane-changing actions cause a drop of capacity in lane 2 which cannot accommodate such high values of flow as the other links. The parameter values for each of the two applied FDs are demonstrated in Figure 4.27.

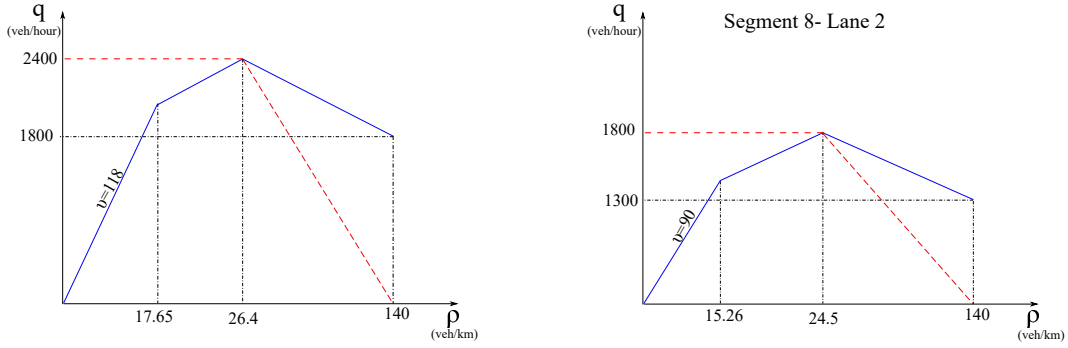


Figure 4.27: Piecewise linear FDs for segment 8 - lane 2 (right) and for the rest of the network (left)

The turning rates required to define the percentage of vehicles that exit the off-ramps are computed based on the respective rates in the no-control case. Since this value might be quite noisy during the simulation we use some smoothing before determining it for the macroscopic model.

4.3.2 Calibrated scenario results

The no-control case refers to the calibrated model described in Section 4.2.2 which is able to reproduce realistic traffic conditions. As it has been detailed before and is also demonstrated in Figure 4.29 the congestion in the case study network and day is initialized due to the increased demand at on-ramp Nieuwerkerk aan den IJssel and a capacity drop appears at segment 10 due to the starting of a strong congestion. These traffic jams spill back where standing queues are also formed due to the lane drop in segment 8 and the congestion covers the stretch up to segment 3 from 6:30 AM until 7:00 AM. From 7:00 AM until 7:30 congestion continues at segment 10 and 9 while the bottlenecks appearing upstream disappear.

Figure 4.28 illustrates the accumulated time spent in the network for the entire simulation period. In the no-control case (red line) the Total Time Spent (TTS) obtained at the end of the simulation is $TTS = 1304$ veh h while the Total Distance Traveled (TDT) is $TDT = 104110$ veh km. Thus, the average speed in the no-control case is $v = 79.8$

km/h. The proposed control scheme that acts every update period leads to $TTS = 1217$ veh h while the total traveled distance is increased due to the applied control actions and is $TDT = 106210$ veh km. The resulted average speed becomes greater than the no-control case scenario and is equal to $v = 87.3$ km/h. This is an improvement of 9.4% on the average speed.

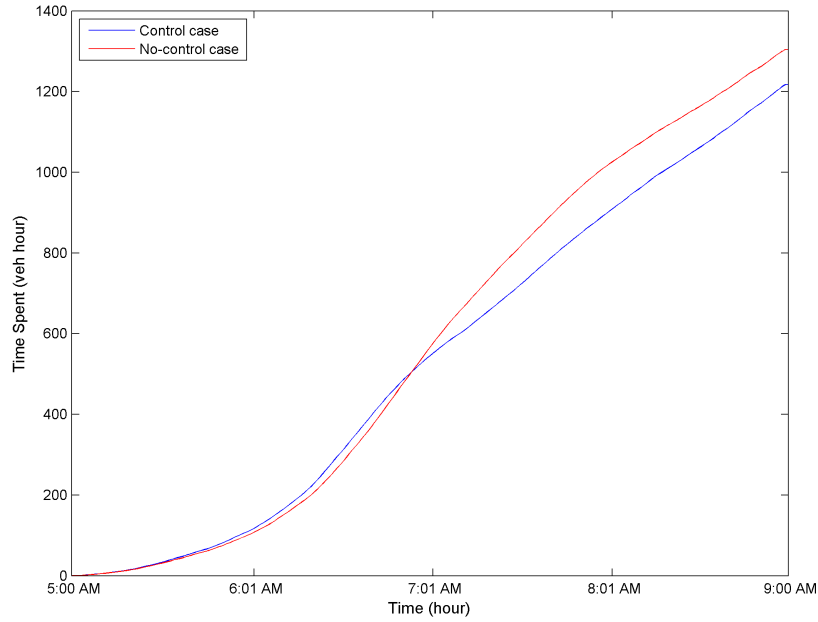


Figure 4.28: Time-accumulated time spent in the control case (blue line) and the no-control case (red line).

The amelioration of the traffic conditions is notable in Figure 4.30 which demonstrates the measured speeds with the MPC scheme enabled. The congestion durates less in lanes 1 and 2 while it is almost eliminated in lane 3. As a matter of fact, the emerged congestion is a consequence of the MTFC actions which aim to achieve capacity flow downstream.

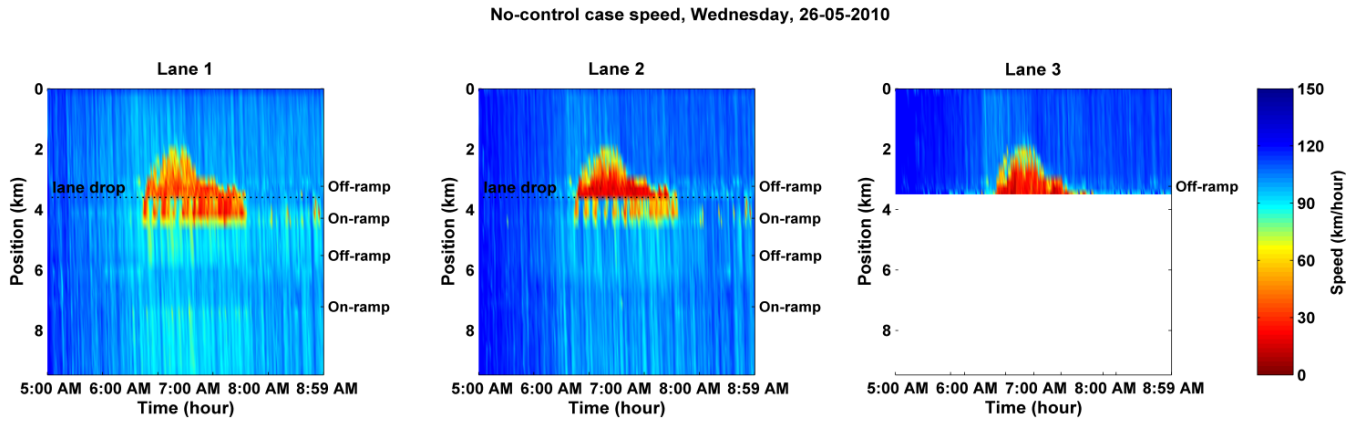


Figure 4.29: No-control case speed, Wednesday 26-05-2010

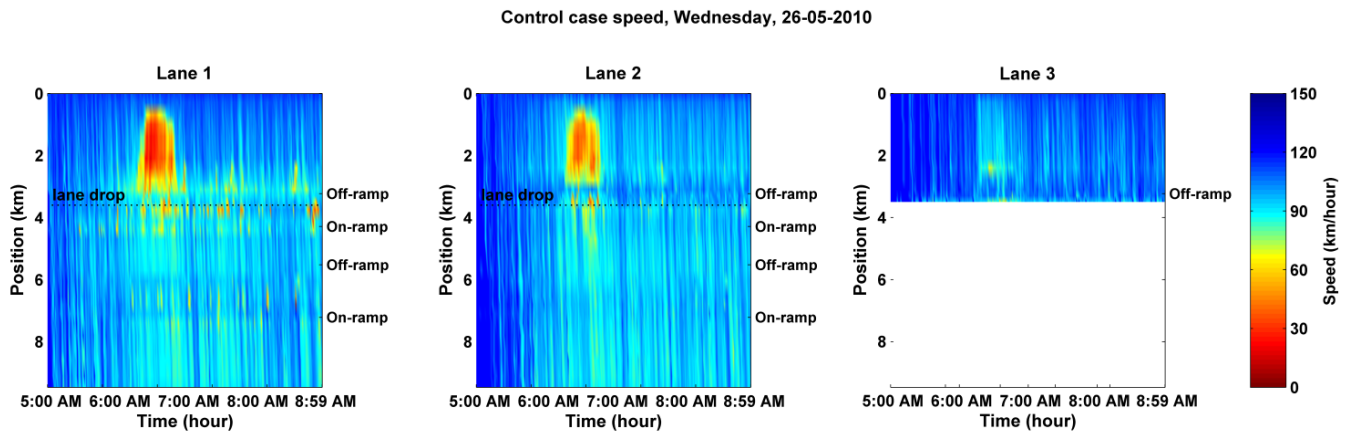


Figure 4.30: Control case speed, Wednesday 26-05-2010

This improvement comes mainly from the mitigation of the congestion-induced capacity drop leading to queue discharge rates lower than the free flow capacity. In the no-control case the capacity drop phenomena appear downstream the segment 10 which contains the on-ramp where congestion is activated. In Figure 4.31 it is clear that the throughput during the congested period is increased due to the applied control strategy.

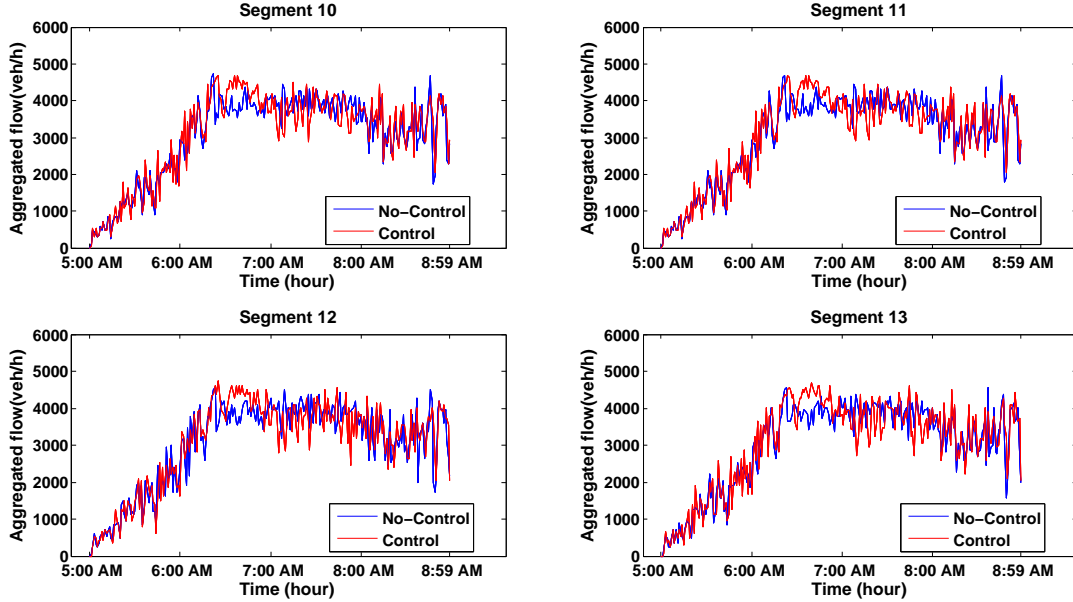


Figure 4.31: Comparison between the aggregate flow in the control (red line) and no-control cases (blue line) at segments 10-13

The control actions that are applied every one minute during the microsimulation are ramp metering, mainstream traffic flow control and lane-changing control. These actions are employed as follows:

- Strong LCC actions are performed in segments 6, 7 and 8 in order to manage to move vehicles from lane 3 to the adjacent lane before they approach the lane-drop location. It has been noticed that in case the vehicles do not change lane before they reach that merging point the creation of queues is unavoidable. In order to create space in lane 2, to accommodate the flow entering from lane 3, lateral movements are also requested from lane 2 to lane 1.
- Due to the aforementioned strong LCC in segments 6,7 and 8 the congestion is almost eliminated in lane 3 but the flow arriving in lanes 1 and 2 has to be decreased. This is achieved via MTFC actions from 6:30 AM until 7:00 AM which limit the flow arriving from upstream by the creation of a controlled congestion. Nevertheless, the speed during these bottlenecks in lanes 2 and 3 has a higher value than the one in

the no-control case.

- The congestion due to the increased demand in Nieuwerkerk aan den IJssel on-ramp is avoided with the application of RM at periods of high flow that enters from the on-ramp. At the same time, LCC actions are employed in segment 9 (the one upstream the segment with the on-ramp) allowing to maintain capacity flow and to avoid significant speed breakdown.
- Left lateral movements are also requested in the segment upstream the on-ramp Moordrecht in order to avoid traffic jams at this location. In parallel, RM actions are also applied in periods with high demand at this on-ramp.

Some of the most important applied control actions are demonstrated in the following Figures 4.32 - 4.41. In particular, the red line plot illustrates the output of the optimization problem adapted to actual applicable control actions while the blue line represents the accomplished actions within the microsimulation.

Lane Changing Control actions: The lateral flows derived from the optimization problem are converted to lane-changing advices sent to the appropriate number of selected vehicles. As it can be seen in Figures 4.32 - 4.34 the flow that actually changes lane during the simulation corresponds pretty well to the requested lateral flows.

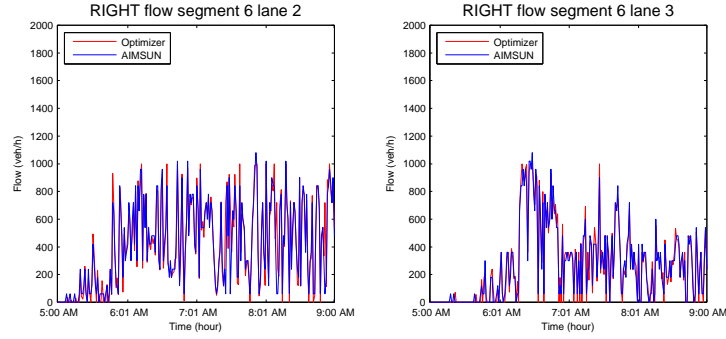


Figure 4.32: Comparison between the requested (red line) and the accomplished (blue line) right lateral movement segment 6

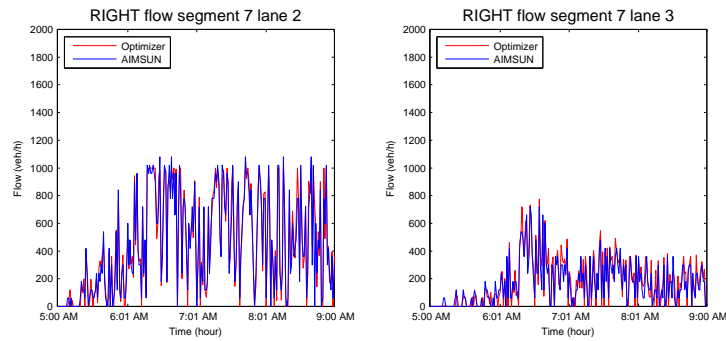


Figure 4.33: Comparison between the requested (red line) and the accomplished (blue line) right lateral movement segment 7

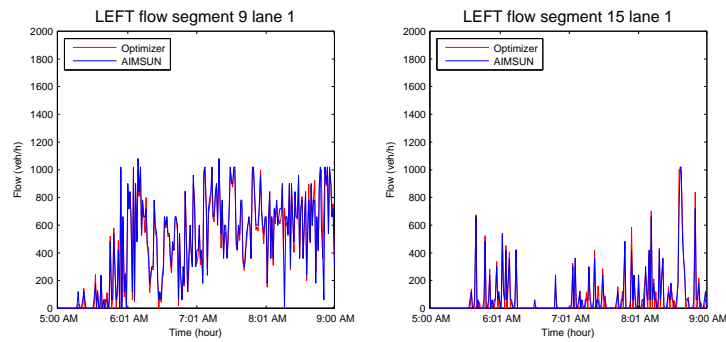


Figure 4.34: Comparison between the requested (red line) and the accomplished (blue line) left lateral movement segments 9 & 15

Mainstream Traffic Flow Control: For the MTFC actions speed limits are imposed with the assumption that all the vehicles can receive specific speed limits based on their location. Note that, although it is clear from Figures 4.35 - 4.37 that there are some discrepancies between the proposed and the actually measured speeds during the microsimulation, Figures 4.38 - 4.40 show that the longitudinal flow is fairly successfully controlled. Additionally, in Figures 4.35 and 4.36 it is visible that some speed reduction is requested in lane 3 at segments 6 and 7 at the beginning of the simulation, while no congestion appears. This leads to an overall deterioration of the total time spent in the network.

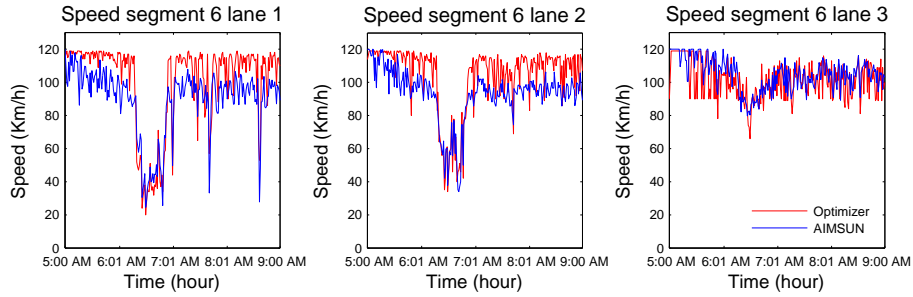


Figure 4.35: Comparison between the requested (red line) and the accomplished (blue line) speed limits in segment 6

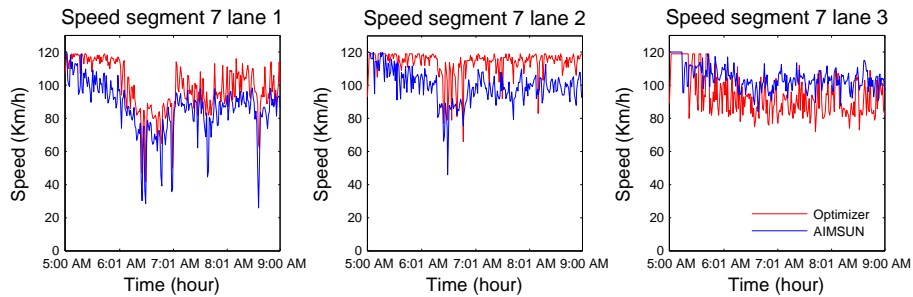


Figure 4.36: Comparison between the requested (red line) and the accomplished (blue line) speed limits in segment 7

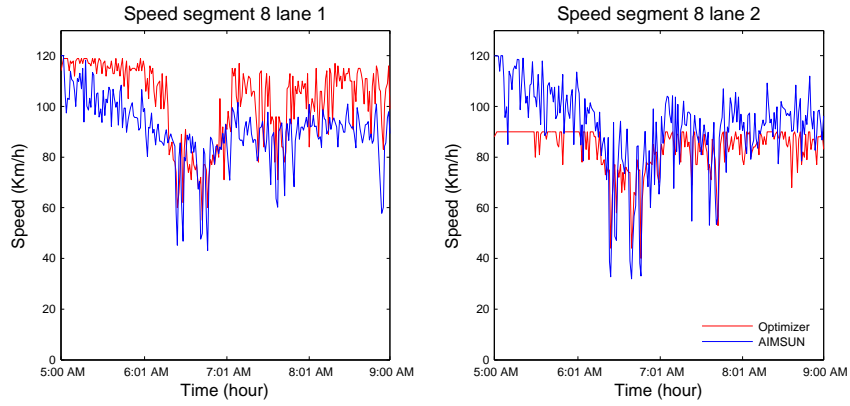


Figure 4.37: Comparison between the requested (red line) and the accomplished (blue line) speed limits in segment 8

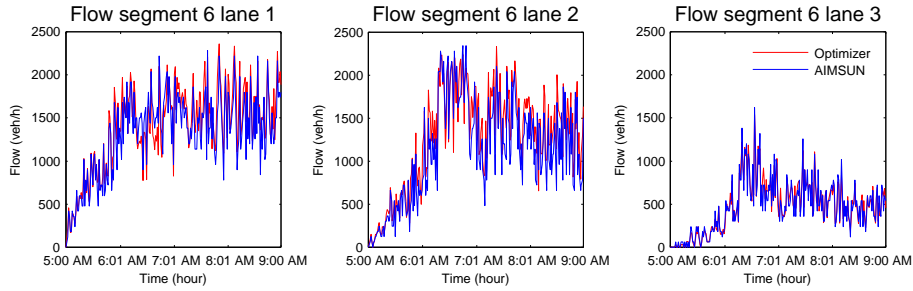


Figure 4.38: Comparison between the expected (red line) and the measured (blue line) longitudinal flow in segment 6

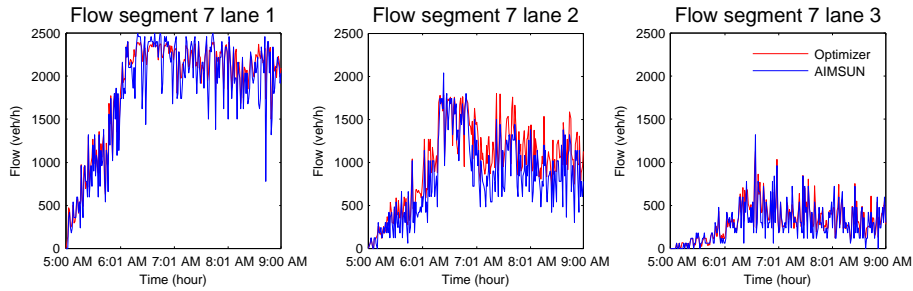


Figure 4.39: Comparison between the expected (red line) and the measured (blue line) longitudinal flow in segment 7

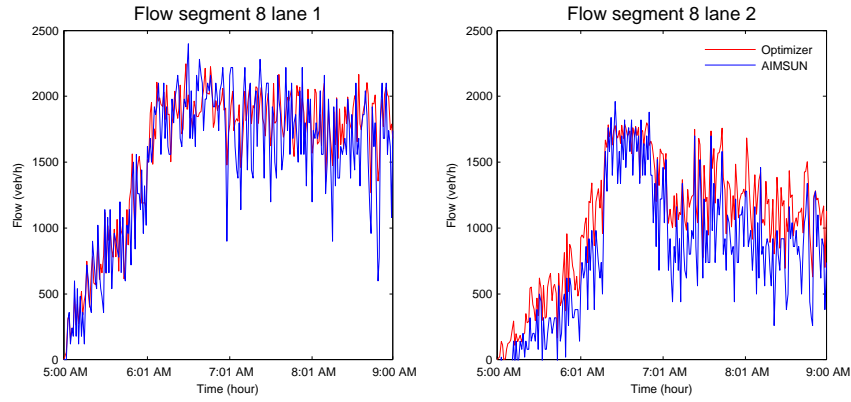


Figure 4.40: Comparison between the expected (red line) and the measured (blue line) longitudinal flow in segment 8

Ramp Metering: The traffic lights placed at the on-ramps control the ramp outflows with the definition of red and green phases based on the resulted ramp outflow from the optimization layer. As illustrated in Figure 4.41 the application of the RM actions is satisfactory and the flow entering from the on-ramps is broadly similar to the control variable $r_{i,j}(k^R)$.

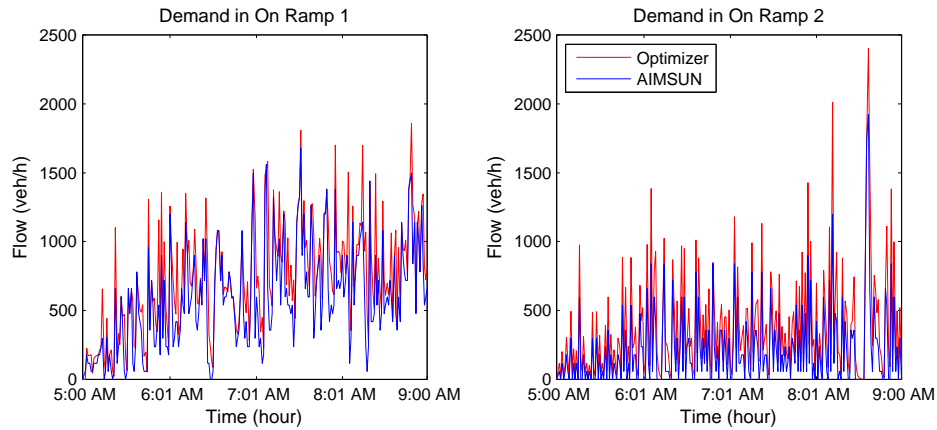


Figure 4.41: Comparison between the requested (red line) and the accomplished (blue line) inflow from on-ramps 1 & 2

4.3.3 Validated scenario results

The calibrated model was also validated in Section (4.2.3) in order to prove that it can produce adequate results with the use of different datasets. The validation test was induced with the use of real data from three different days but the proposed control strategy will be examined only for “Monday 08-06-2009”. The traffic conditions in the investigated day are quite similar to the conditions of the calibrated model. Congestion starts at on-ramp Nieuwerkerk aan den IJssel and propagates upstream from 06:20 AM until 07:00 AM.

The application of the MPC in the microscopic model using a validated scenario, results also in an improvement of the average speed. In Figure 4.42 the time accumulated time spent is illustrated. In the no-control case the Total Time Spent at the network is $TTS = 1270$ veh h and the Total Distance Traveled is $TDT = 100610$ veh km. The application of the MPC scheme in the microsimulation leads to a reduction of the total time spent which becomes $TTS = 1215$ veh h while the total distance traveled is increased to $TDT = 102430$ veh km. The average speed is equal to $v = 79.2$ km/h in the no-control case and $v = 84.3$ km/h in case the control framework is applied. This corresponds to an improvement of 6.4% on the average speed.

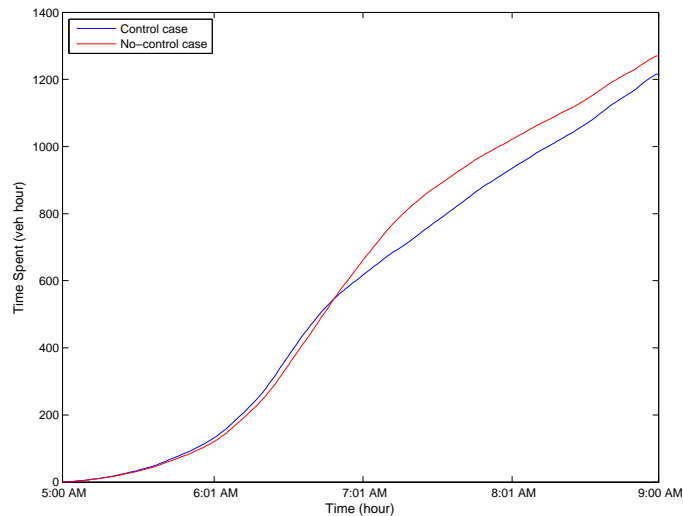


Figure 4.42: Time-accumulated time spent in the control case (blue line) and the no-control case (red line) on Monday 08-06-2009

Figures 4.43 and 4.44 illustrate the measured speeds in the no-control and in the control case scenarios respectively. The control actions result in the elimination of congestion in lane 3 while in lanes 1 and 2 traffic jams are created due to MTFC. These controlled bottleneck which is a consequence of the control strategy lasts from 06:20 AM until 06:40 AM in lane 2 while in lane 1 there is some speed reduction at the segment with the on-ramp and in the upstream until the end of the simulation.

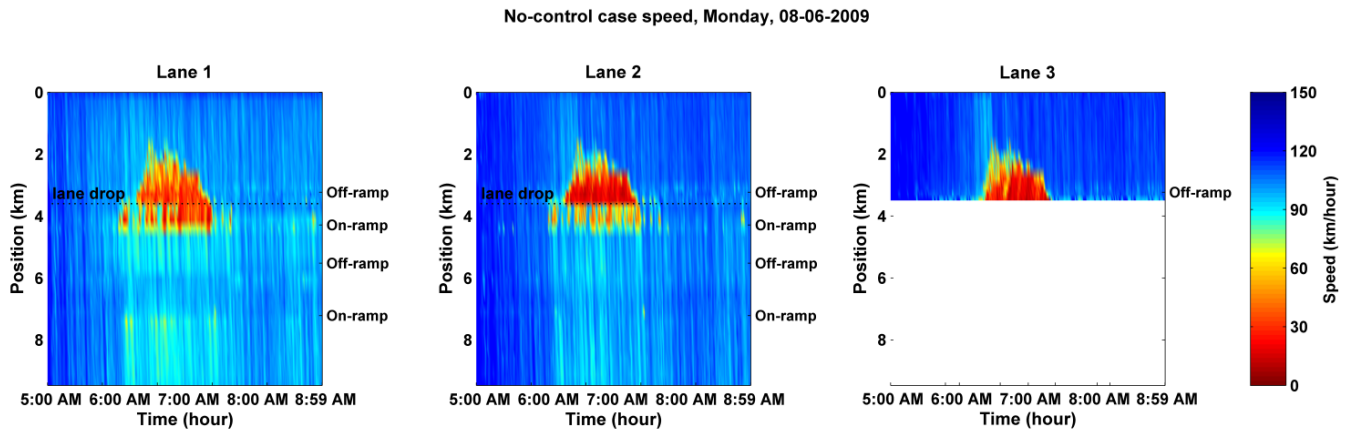


Figure 4.43: No-control case speed, Monday 08-06-2009

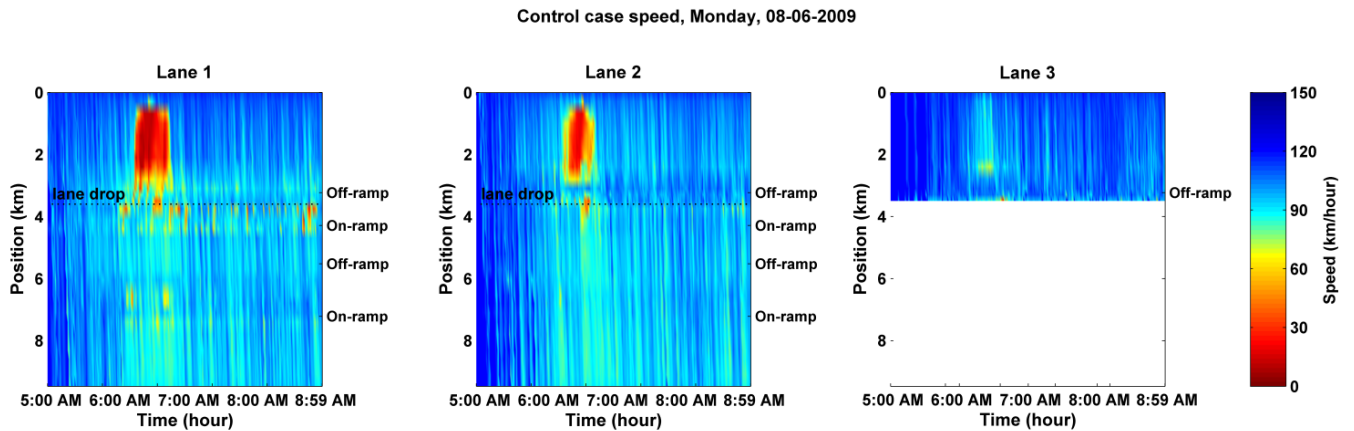


Figure 4.44: Control case speed, Monday 08-06-2009

Chapter 5

Conclusions and future work

5.1 Conclusions

The objective of this master thesis was to evaluate a control strategy on a multilane network with diverse characteristics. To this end, a calibration and validation process of AIMSUN microscopic simulator was carried out in the first part of this work. In the second part the application of an MPC strategy proposed by Roncoli et al. (2014) on the calibrated model was tested. The case study site is a part of the freeway A20 which connects Rotterdam to Gouda in the Netherlands. The quite complex infrastructure features of the network were developed with precision in the microsimulator while detailed real data flow and speed measurements were used in order to tune the microscopic model parameters. The dynamic scenario of the simulation was based on the real dataset that was chosen for the model's calibration while other demand profiles were used to further assess the validity of the model. It was proved that the selected parameters set in the microscopic simulation model can lead to realistic behavior. Not only the output speed pattern was well matched with the real one but also significant traffic phenomena were realistically replicated. The calibrated model was additionally validated and it was proved that the calibrated parameters can lead to realistic results for different dynamic scenarios which are defined using other real datasets.

Subsequently, the calibrated model served as a reference case in order to test the

proposed control scheme and evaluate its efficiency. Ramp metering, mainstream traffic flow control and lane changing control were the integrated actions of the applied strategy with the assumption that all the simulated flow was equipped with VACS. The MPC approach resulted in an improvement of traffic congestion in the case study network with an improvement of 9.4% on the average speed. Additionally, the given control actions were in overall accomplished except from some minor cases that there were discrepancies between the requested and the actual performed actions from the vehicles. This control strategy was also used for the mitigation of traffic congestion for one of the different scenario cases used in the validation procedure. The outcome of this employment was also satisfactory with an amelioration of the average speed in the network equal to 6.4%.

5.2 Future work

Although this study has shown that the application of an MPC scheme on a multilane model with complex infrastructure can lead to an amelioration of the traffic conditions more work needs to be done to get further improvement on the overall performance. As it is also visible in Figures 4.28 and 4.42 a source of TTS degradation is the application of control actions in uncongested conditions due to imprecise measurements, model mismatch or inaccurate numerical approximations. Even though, the overall time spent in the network is reduced when the MPC framework is applied, the time spent at the beginning of the simulation where no bottlenecks appear is higher due to the applied control actions. To overcome this, a definition of an activation/deactivation logic can be introduced. This would permit to apply control only when its is necessary, leaving the system uncontrolled when control actions are not needed. More broadly, another aspect that has to be treated is the consideration of mixed traffic conditions. The introduction of different types of vehicles in the simulated flow including vehicles equipped with VACS and manually driven vehicles could lead to a more realistic approach concerning the proposed control strategy.

Bibliography

- Baskar, L. D., B. D. Schutter, and H. Hellendoorn (2012). Traffic management for automated highway systems using model-based predictive control. *IEEE Transactions on Intelligent Transportation Systems* 13(2), 838–847.
- Burger, M., M. V. D. Berg, A. Hegyi, B. D. Schutter, and J. Hellendoorn (2013). Considerations for model-based traffic control. *Transportation Research Part C: Emerging Technologies* 35, 1–19.
- Chevallier, E. and L. Leclercq (2009). Do microscopic merging models reproduce the observed priority sharing ratio in congestion? *Transportation Research Part C: Emerging Technologies* 17(3), 328–336.
- Chu, L., H. Liu, J.-S. Oh, and W. Recker (2004). A calibration procedure for microscopic traffic simulation. In *Proceedings of the 2004 TRB Annual Meeting*.
- Deep, K., K. P. Singh, M. Kansal, and C. Mohan (2009). A real coded genetic algorithm for solving integer and mixed integer optimization problems. *Applied Mathematics and Computation* 212(2), 505–518.
- Diakaki, C., M. Papageorgiou, I. Papamichail, and I. Nikolos (2015). Overview and analysis of vehicle automation and communication systems from a motorway traffic management perspective. *Transportation Research Part A: Policy and Practice* 75, 147–165.
- FHWA (2004). Traffic analysis toolbox volume iii: Guidelines for applying traffic microsimulation software. Technical report, Washington D.C, USA: FHWA-HRT-04-040.

- FHWA, U.S. Department of Transportation (1997). *CORSIM User's Manual*. FHWA, U.S. Department of Transportation.
- Gipps, P. (1981). A behavioural car-following model for computer simulation. *Transportation Research Part B: Methodological* 15(2), 105–111.
- Gipps, P. (1986). A model for the structure of lane-changing decisions. *Transportation Research Part B: Methodological* 20(5), 403–414.
- Goldberg, D. E. (1989). *Genetic algorithms in search, optimization, and machine learning*. Addison-Wesley Publishing Co.
- Gurobi (2013). *Gurobi optimizer reference manual*. Huston.
- Hegyi, A., B. D. Schutter, and H. Hellendoorn (2005). Model predictive control for optimal coordination of ramp metering and variable speed limits. *Transportation Research Part C: Emerging Technologies* 13(3), 185–209.
- Holland, J. H. (1992). *Adaptation in natural and artificial systems: an introductory analysis with applications to biology, control, and artificial intelligence*. MIT Press.
- Hourdakis, J., P. Michalopoulos, and J. Kottommannil (2003). Practical procedure for calibrating microscopic traffic simulation models. *Transportation Research Record: Journal of the Transportation Research Board* 1852, 130–139.
- Kesting, A. and M. Treiber (2008). Calibrating car-following models by using trajectory data: Methodological study. *Transportation Research Record: Journal of the Transportation Research Board* 2088, 148–156.
- Kim, K., J. V. Medanić, and D. I. Cho (2008). Lane assignment problem using a genetic algorithm in the automated highway systems. *International Journal of Automotive Technology* 9(3), 353–364.

- Lagarias, J. C., J. A. Reeds, M. H. Wright, and P. E. Wright (1998). Convergence properties of the nelder–mead simplex method in low dimensions. *SIAM Journal on Optimization* 9(1), 112–147.
- Liu, H., X. Yang, and J. Sun (2006). Parameter calibration for vissim using a hybrid heuristic algorithm: A case study of a congested traffic network in china. *Applications of Advanced Technology in Transportation*.
- MATLAB (2014). *Global Optimization Toolbox*. The MathWorks Inc.
- Messner, A. and M. Papageorgiou (1990). Metanet: A macroscopic simulation program for motorway networks. *Traffic Engineering & Control* 31(8-9), 466–470.
- Panwai, S. and H. Dia (2005). Comparative evaluation of microscopic car-following behavior. *IEEE Transactions on Intelligent Transportation Systems* 6(3), 314–325.
- Papageorgiou, M. (2004). Overview of road traffic control strategies. In *Proceedings. 2004 International Conference on Information and Communication Technologies: From Theory to Applications, 2004*.
- Papageorgiou, M., C. Diakaki, V. Dinopoulou, A. Kotsialos, and Y. Wang (2003). Review of road traffic control strategies. *Proceedings of the IEEE* 91(12), 2043–2067.
- Papageorgiou, M. and I. Papamichail (2008). Overview of traffic signal operation policies for ramp metering. *Transportation Research Record: Journal of the Transportation Research Board* 2047, 28–36.
- Papamichail, I., A. Kotsialos, I. Margonis, and M. Papageorgiou (2010). Coordinated ramp metering for freeway networks – a model-predictive hierarchical control approach. *Transportation Research Part C: Emerging Technologies* 18(3), 311–331.
- Park, B. B. and H. M. Qi (2005). Development and evaluation of a procedure for the calibration of simulation models. *Transportation Research Record: Journal of the Transportation Research Board* 1934, 208–217.

- Park, Byungkyu, H. (2006). Microscopic simulation model calibration and validation for freeway work zone network - a case study of vissim. *2006 IEEE Intelligent Transportation Systems Conference*.
- PTV Planug Transport Verkehr AG. Innovative Transportation Concepts LLC (2001). *VISSIM Version 3.6 Manual*. PTV Planug Transport Verkehr AG. Innovative Transportation Concepts LLC.
- Roncoli, C., M. Papageorgiou, and I. Papamichail (2015a). Traffic flow optimisation in presence of vehicle automation and communication systems – Part I: A first-order multi-lane model for motorway traffic. *Transportation Research Part C: Emerging Technologies* 57, 241–259.
- Roncoli, C., M. Papageorgiou, and I. Papamichail (2015b). Traffic flow optimisation in presence of vehicle automation and communication systems – Part II: Optimal control for multi-lane motorways. *Transportation Research Part C: Emerging Technologies* 57, 260–275.
- Roncoli, C., I. Papamichail, and M. Papageorgiou (2014). Model predictive control for multi-lane motorways in presence of VACS. In *Proceedings 17th International IEEE Conference on Intelligent Transportation Systems*, pp. 501–507.
- Roncoli, C., I. Papamichail, and M. Papageorgiou (2016). Hierarchical model predictive control for multi-lane motorways in presence of vehicle automation and communication systems. *Transportation Research Part C: Emerging Technologies* 62, 117–132.
- Schakel, W. J. and B. V. Arem (2014). Improving traffic flow efficiency by in-car advice on lane, speed, and headway. *IEEE Trans. Intell. Transport. Syst. IEEE Transactions on Intelligent Transportation Systems* 15(4), 1597–1606.
- Spiliopoulou, A., M. Kontorinaki, M. Papageorgiou, and P. Kopelias (2014). Macroscopic traffic flow model validation at congested freeway off-ramp areas. *Transportation Research Part C: Emerging Technologies* 41, 18–29.

- Toledo, T., H. Koutsopoulos, A. Davol, M. Ben-Akiva, W. Burghout, I. Andréasson, T. Johansson, and C. Lundin (2003). Calibration and validation of microscopic traffic simulation tools: Stockholm case study. *Transportation Research Record: Journal of the Transportation Research Board* 1831, 65–75.
- Transport Simulation Systems (2014). *Aimsun 8 Dynamic Simulators Users' Manual*. Transport Simulation Systems.
- Treiber, M., A. Hennecke, and D. Helbing (2000). Congested traffic states in empirical observations and microscopic simulations. *Physical Review E* 62(2), 1805–1824.
- Vanderwerf, J., S. Shladover, N. Kourjanskaia, M. Miller, and H. Krishnan (2001). Modeling effects of driver control assistance systems on traffic. *Transportation Research Record: Journal of the Transportation Research Board* 1748, 167–174.
- Varaiya, P. (1993). Smart cars on smart roads: problems of control. *IEEE Transactions on Automatic Control* 38(2), 195–207.
- Wang, J., R. Liu, and F. Montgomery (2005). Car-following model for motorway traffic. *Transportation Research Record: Journal of the Transportation Research Board* 1934, 33–42.
- Zhizhou, W., S. Jian, and Y. Xiaoguang (2005). Calibration of vissim for shanghai expressway using genetic algorithm. In *Proceedings of the 2005 Winter Simulation Conference*, edited by M. E. Kuhl, N. M. Steiger, F. B. Armstrong, and J. A. Joines.